COMILLAS
UNIVERSIDAD PONTIFICIA
ICAI

Grado en Ingenería en Tecnologías Industriales

Trabajo Fin de Grado

Investigating Electromagnetic Vibration Energy Harvesters

Author: Guillermo Costillo Salgado

Supervisor: Professor Rasmus Bjørk

Madrid

June 2021

Declaro, bajo mi responsabilidad, que el Proyecto presentado con el título

"*Investigating Electromagnetic Vibration Energy Harvesters"*

en la ETS de Ingeniería - ICAI de la Universidad Pontificia Comillas en el curso académico "*2020-2021* " es de mi autoría, original e inédito y no ha sido presentado con anterioridad a otros efectos. El Proyecto no es plagio de otro, ni total ni parcialmente y la información que ha sido tomada de otros documentos está debidamente referenciada.

Fdo.: *Guillermo Costillo Salgado* Fecha: *23/ 06 / 2021*

Autorizada la entrega del proyecto

EL DIRECTOR DEL PROYECTO

Fdo.: *Rasmus Bjørk* Fecha: *23/06/2021*

Rasmus Bjørk

Grado en Ingeniería en Tecnologías Industriales

Trabajo Fin de Grado

Investigating Electromagnetic Vibration Energy Harvesters

Author: Guillermo Costillo Salgado

Supervisor: Professor Rasmus Bjørk

Madrid

June 2021

Estudio de recolectores de energía electromagnéticos a través de las vibraciones

Autor: Guillermo Costillo Salgado.
Director: Rasmus Bjørk.
Entidad Colaboradora: Universidad Técnica de Dinamarca (DTU).

RESUMEN DEL PROYECTO

El cambio de baterías de los dispositivos inalámbricos es un gran problema para la red del Internet de las Cosas (IoT por sus siglas en inglés). Para contribuir a la solución de este problema, este proyecto presenta un diseño en forma de péndulo esférico de un recolector electromagnético de energía a través de las vibraciones y el estudio posterior de su comportamiento. El recolector pretende ser en 2D, sin pérdidas mecánicas y que pueda obtener energía en una amplia banda de vibraciones a bajas frecuencias.

1 Introducción

Se espera que el Internet de las Cosas crecerá significativamente en los próximos años, lo que implica una gran cantidad de dispositivos inalámbricos en funcionamiento, cuyas baterías deben cambiarse regularmente. [1] Este cambio de baterías se traduce en un alto coste económico y medioambiental. Para resolver este problema, se están desarrollando diferentes tecnologías de recolección de energía. Se trata de tecnologías que obtienen energía del entorno a pequeña escala para alimentar dispositivos de baja potencia.

Las principales fuentes disponibles en el entorno para la captación de energía son la solar, los gradientes térmicos, la radiofrecuencia y el movimiento en forma de vibraciones. Cada fuente tiene sus ventajas e inconvenientes y, dependiendo de la situación, una u otra puede ser mejor, pero la más flexible y fácil de encontrar en el entorno es el movimiento en forma de vibraciones.

Hay dos tecnologías principales para la recoleción de energía a través de las vibraciones: Los generadores piezoeléctricos (PGs) y los recolectores electromagnéticos. Dado que los PGs tienen la gran desventaja de la degradación del material a través del tiempo [2], este proyecto

se centrará en los recolectores electromagnéticos. Ellos se basan en la Ley de Faraday por la que se busca un movimiento relativo entre imanes y bobinas para inducir un voltaje alterno.

En la literatura se han encontrado diferentes tecnologías de recolectores electromagnéticos. Algunas de ellas eran muy eficientes con altas densidades de potencia, sin embargo eran muy dependientes de la frecuencia de resonancia lo que resultaba en una limitación en la banda de frecuencias [3] [4]. Algunos autores lograron resolver este problema utilizando recolectores de diseño en forma de péndulos con ajuste de frecuencia [5]. Todos los recolectores encontrados en la literature son diseñados para la obtención de energía desde vibraciones en únicamente una dimensión, sin embargo, algunas vibraciones aparecen en 2D, lo que significa una pérdida potencial de energía recolectada.

De este modo, este trabajo pretende estudiar un recolector electromagnético de 2D diseñado por el estudiante de doctorado Carlos Imbaquingo, y encontrar soluciones o alternativas para el problema de la fricción detectado en estudios anteriores. Esta evaluación experimental condujo a la idea de construir otro recolector que consiste en un péndulo esférico. Se trata de un diseño simple en 2D, sin fricción, que puede obtener energía en una amplia banda de bajas frecuencias. Se probarán y compararán diferentes configuraciones del recolector.

2 Diseño del recolector de energía

El diseño conceptual del recolector de energía consiste en una bobina de cobre que cuelga de un hilo conectado a un punto fijo relativo a una base en forma de cuenco. Esta base contiene imanes insertados en su superficie. Cuando la bobina oscila con respecto a la base debido a la vibración horizontal del cuenco, se provoca un campo magnético variable a través de las bobinas y, por tanto, se produce una tensión alterna.

Las ecuaciones de movimiento se derivaron con usando la mecánica Newtoniana con ayuda de las matrices de Euler y resultaron ser:

$$i_2 : I_t \cdot \ddot{\theta} + (I_e - I_t) \cdot sin\theta \cdot \dot{\phi} \cdot cos\theta \cdot \dot{\phi} = r \cdot (F_x \cdot cos\phi + F_y \cdot sin\phi - C \cdot \dot{\theta}) \tag{1}$$

$$j_2 : I_t \cdot (\dot{\theta} \cdot cos\theta \cdot \dot{\phi} + \ddot{\phi} \cdot sin\theta) + (I_t - I_e) \cdot \dot{\theta} \cdot cos\theta \cdot \dot{\phi} = -r \cdot (F_x \cdot cos\theta \cdot sin\phi + F_y \cdot cos\phi \cdot cos\theta - C \cdot sin\theta \cdot \dot{\phi}) \tag{2}$$

$$k_2 : I_e \cdot (-\dot{\theta} \cdot sin\theta \cdot \dot{\phi} + \ddot{\phi} \cdot cos\theta) = 0 \tag{3}$$

Las ecuaciones fueron desarrolladas para encontrar un modelo analítico del sistema, sin embargo, como se priorizó la realización de experimentos, no quedó tiempo para el modelo analítico.

El prototipo fue impreso en 3D en PLA con una impresora "Ultimaker 3" debido a la versatilidad de la técnica. Se diseñaron tres configuraciones diferentes. Todas ellas implicaban una base con 29 imanes de neodimio fijados en ella. Tenían un grosor de 5 mm y un diámetro de 9 mm con un grado de magnetización igual a N50 [6]. La orientación de los imanes se eligió en un intento de maximizar el flujo magnético variable a través de las bobinas alternando orientaciones norte y sur radialmente como se puede ver en la figura 1.

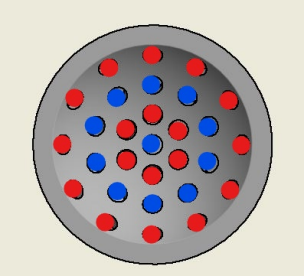

Figure 1: Orientación de los imanes en la base visto desde arriba. Rojo muestra el sur y azul, el norte.

Las tres configuraciones pueden verse en la figura 2. La más sencillas consiste en una bobina que cuelga de una cuerda desde un punto fijo conectado a la base. La bobina es de hilo de cobre con una resistencia interna e inductancia de 1,6 y 0,35mH respectivamente. Tiene una altura de 10 mm y un diámetro interior de 18 mm y exterior de 25 mm. Una configuración más compleja se realizó diseñando un soporte para las bobinas en el que oscilaban cuatro bobinas conectadas en serie. En este caso, las bobinas elegidas eran más esbeltas que las anteriores, por lo que se distribuían mejor en el soporte. Esta configuración se pensó para que pudiera pasar más flujo por las bobinas, generando en principio más potencia. El último diseñp consistía en ocho bobinas en serie en un intento de obtener aún más energía que con las configuraciones de 4 bobinas.

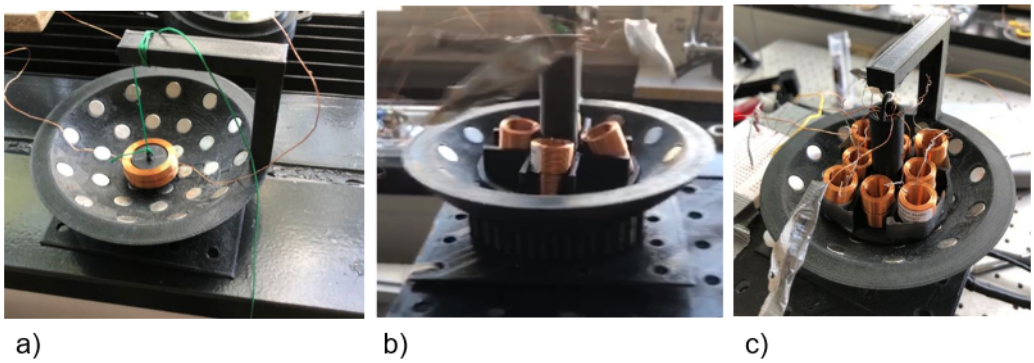

Figure 2: Diferentes configuraciones del prototipo. a)1 bobina b) 4 bobinas c) 8 bobinas

3 Metodología

Todos los experimentos se realizaron siguiendo el mismo procedimiento: Se utilizó un agitador electrodinámico bidimensional "H2W technologies" para generar las vibraciones. Se controló mediante una interfaz LabVIEW. La tensión de salida fue registrada por un sistema de Adquisición y Control de Datos (DAC) de National Instruments (NI USB-6351) de 16 canales. Los datos de salida fueron leídos desde MatLab. (Ver figura 3).

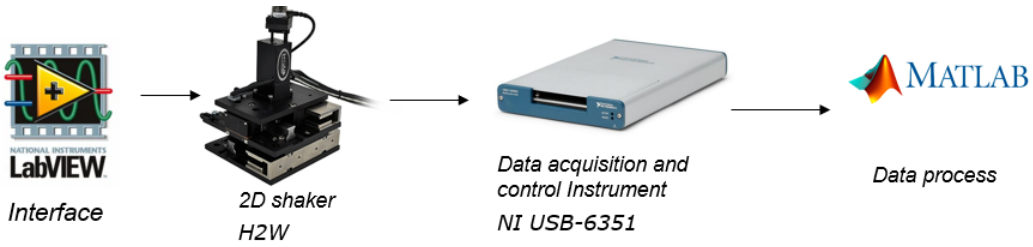

Figure 3: Methodology followed to make the experiments

Los experimentos se realizaron con diferentes características de vibración en amplitude y frequencía en 1D y 2D. Aunque los experimentos en circuito abierto no aportan información práctica porque no se obtiene potencia, todos ellos se hicieron de esa manera para ver el límite del sistema. Además, para los ajustes de vibración del agitador en los que se produjo la máxima tensión de salida en cada diseño de dispositivo, se repitieron los experimentos conectando la carga que maximiza la potencia de salida, que es equivalente a la resistencia interna del sistema. Esto se hizo para comparar la máxima potencia obtenida en cada una las diferentes configuraciones.

4 Resultados

La figura 4 muestra la media cuadrática (RMS por sus siglas en inglés) de la tensión de las diferentes configuraciones en el estudio en una dimensión. Se puede observar como la frecuencia natural del sistema son 2Hz ya que en ella se encuentra un máximo de tensión. Además, la tensión tiende a aumentar con la amplitud, lo que era de esperar porque el desplazamiento de las bobinas aumenta a medida que lo hace la esta.

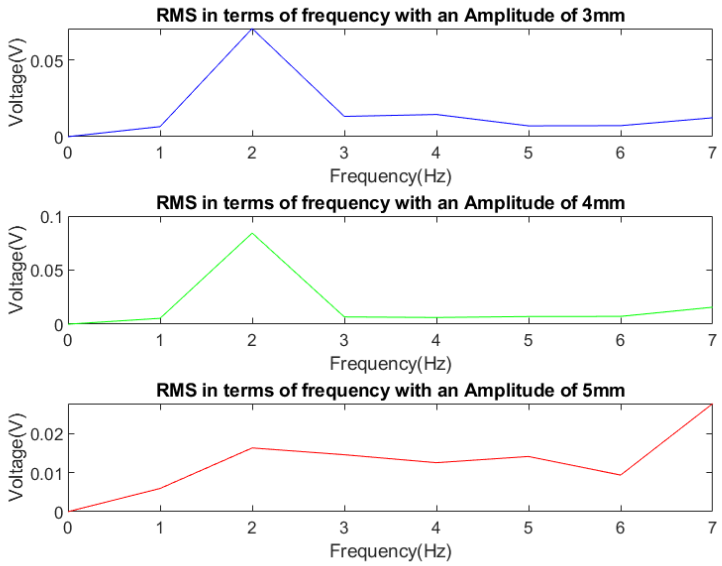

Figure 4: RMS en función de la frecuencia para distintas amplitudes con vibraciones en una dimensión.

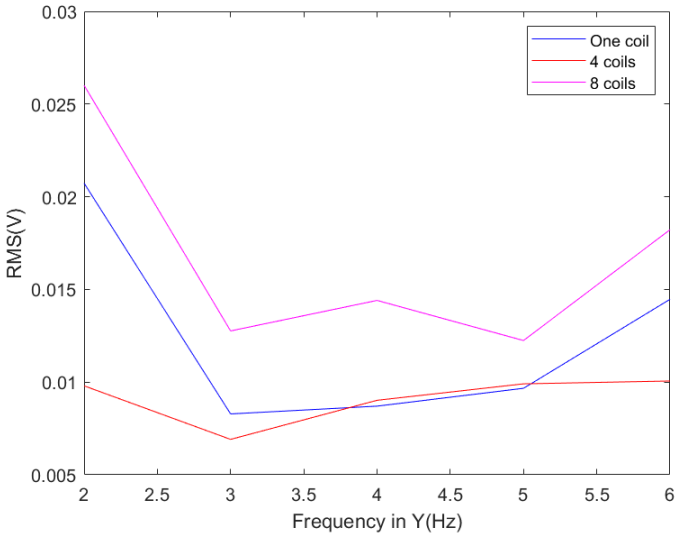

Figure 5: RMS con vibraciones en 2D. En el eje "x": amplitud constante de 3 mm y frecuencia de 3 Hz. En el eje "y", amplitud constante de 4 mm and frequencía cambiante de 2 a 6 Hz.

Se observa que la configuración de 1 bobina proporcionó casi el mismo RMS que la de 8 bobinas e incluso más que el diseño de 4 bobinas. Esto puede deberse a dos cosas diferentes. En primer lugar, las bobinas utilizadas para 4 y 8 bobinas son más delgadas, por lo que se concentran menos vueltas cerca de la superficie de la base, donde aparece la mayor parte de la intensidad del flujo. En segundo lugar, como las bobinas están conectadas en serie, su tensión puede estar desfasada, anulándose mutuamente y provocando una menor tensión de salida.

La figura 5 muestra el RMS de todos los experimentos en 2D. Los resultados de las vibraciones 2D son similares a los de 1D.

La figura 6 muestra la potencia máxima y el RMS máximo en cada configuración con la carga óptima en cada caso. La potencia obtenida se calcula de la siguiente manera:

$$P = \frac{U_{rms}^2}{R} \tag{4}$$

donde R es la carga.

La máxima potencia obtenida es 177 μW, con la configuración de una bobina. Esto puede ser debido a tres cosas. En primer lugar, la baja resistencia interna hace un recolector mucho más eficiente. Segundo, la bobina en esta configuración es menos delgada, por lo que hay

más vueltas cerca de la superficie, donde aparece la mayor parte del flujo magnético. Y tercero, porque en las configuraciones de 4 y 8 bobinas, la tensión en cada una de ellas puede estar desfasada, lo que reduce la tensión total.

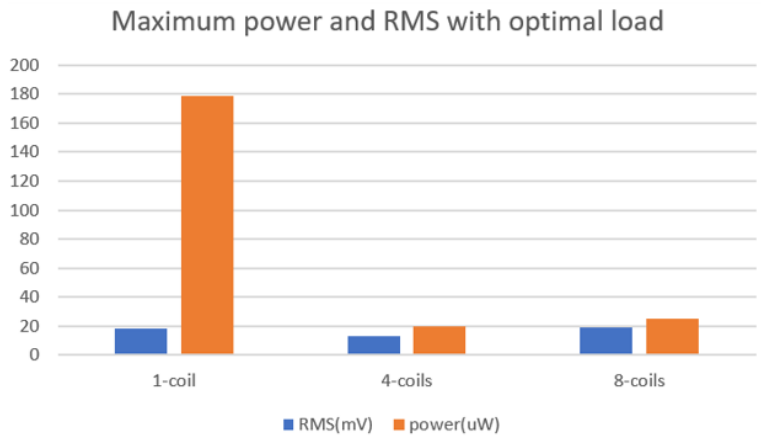

Figure 6: Máxima potencia y RMS obtenida en cada diseño con la carga óptima. Las características de vibración son las siguientes: amplitud (x=5,y=0)mm, frecuencia (x=2,y=0)Hz para los diseños de 2 y 4 bobinas. Amplitud(x=3,y=4)mm, frecuencia(x=3,y=2)Hz para el diseó de una bobina.

5 Conclusiones

Este proyecto presenta el diseño de un péndulo esférico de un recolector electromagnético de energía a través vibraciones y los experimentos realizados para estudiar su comportamiento. Se muestra cómo la configuración óptima tiende a ser la de menor resistencia interna. Se logran los objetivos de encontrar un recolector 2D sin fricción mecánica. La máxima potencia obtenida fue suficiente para alimentar dispositivos de muy baja potencia. El sistema podría mejorarse aumentando la intensidad del flujo magnético a través de las bobinas.

6 Referencias

[1] Michael Vedomske. Without device longevity, the internet of things will never be.URLhttps://medium.co
the-grand-vision-of-the-internet-of/without-device-longevity-the-internet-of-things-will-never-
be-58c904703abb: :text

[2] BP Mann and ND Sims. Energy harvesting from the nonlinear oscillations of magneti-
clevitation.Journal of sound and vibration, 319(1-2):515–530, 2009.

[3] Krzysztof Kecik, Andrzej Mitura, Stefano Lenci, and Jerzy Warminski. Energy harvesting from a magnetic levitation system.International Journal of Non-Linear Mechanics,94:200–206, 2017.

[4] Davide Castagnetti. A simply tunable electromagnetic pendulum energy harvester.Meccanica, 54(6):749–760, 2019.

[5] Magnetic properties of neudymium magnets. URLhttps://www.magnetexpert.com/magnetic-properties-of-neodymium-magnets-i694.

[6] R Salazar, M Serrano, and A Abdelkefi. Fatigue in piezoelectric ceramic vibrationalenergy harvesting: A review.Applied Energy, 270:115161, 2020.

Investigating Electromagnetic Vibration Energy Harvesters

Author: Guillermo Costillo Salgado.
Supervisor: Rasmus Bjørk.
Collaborating entity: Denmark Technical University (DTU).

Abstract

The battery replacement of the wireless devices is a big issue for the IoT network. To contribute in the solution of this problem, this project presents an spherical pendulum design of an electromagnetic vibration energy harvester and the posterior study of its behaviour. The harvester aims to be in 2D with no mechanical losses and which can obtain energy in a broad band of low frequencies.

1 Introduction

The Internet of Things network is expected to grow significantly in the following years, meaning a great amount of wireless devices into work, which batteries need to be changed regularly. [1] This battery replacement translates as a high economical and environmental cost. To solve this problem, different energy harvesting technologies are being developed. They consists of technologies that obtain energy from the environment in small scale for powering low power devices.

The main sources available in the environment for energy harvesting are solar, thermal gradients, radio frequency and motion in the form o vibrations. Each source has its advantages and disadvantages and depending on the situation, one or another could be better, however, the most flexible and easily found in the environment is the motion in the form of vibrations.

There are two main technologies for harvesting energy from vibrations: Piezoelectric Generators (PGs) and Electromagnetic vibration energy harvesters (EMVEHs). Since the PGs has the major disadvantage of the degradation of the material through time [2], this project will focus on the EMVEHs. They work using the Farady´s law and look for a relative motion between magnet and coils to induce alternating voltage in the coils.

Different EMVEHs technologies have been found in the literature. Some of them where very efficient with high power densities, however were very dependent on the resonant frequency resulting on a limitation in the band of frequencies [3] [4]. Some authors managed to solve this problem using pendulum-design harvesters with frequency tuning [5]. All the harvesters were designed for harvesting energy just from 1D vibrations, however, some vibrations appear in 2D, meaning a loss of potential harvest.

In that way, this work aims to study a 2D EMVEH designed by the Phd candidate Carlos Imbaquingo, and find solutions or alternatives for the friction problem, which was detected in previous studies. This experimental assessment lead to the idea of building another harvester consisting of an spherical pendulum. It aims to be a simple 2D architecture, with no friction, that can harvest energy in a broad band of low frequencies. Different configurations of the harvester will be tested and compared.

2 Spherical Pendulum harvester

The conceptual design of the harvester consists of a coil made of copper wire hanging by a thread connected to a fixed point relative to a bowl-shaped base. This base contains magnets inserted in its surface. When the coil swings relative to the base due to the horizontal vibration of the bowl, a variable magnetic field across the coils is provoked,and therefore, an alternating voltage is produced.

The equations of motion were derived using Newton-Euler´s equations and resulted to be:

$$i_2 : I_t \cdot \ddot{\theta} + (I_e - I_t) \cdot sin\theta \cdot \dot{\phi} \cdot cos\theta \cdot \dot{\phi} = r \cdot (F_x \cdot cos\phi + F_y \cdot sin\phi - C \cdot \dot{\theta}) \tag{5}$$

$$j_2 : I_t \cdot (\dot{\theta} \cdot cos\theta \cdot \dot{\phi} + \ddot{\phi} \cdot sin\theta) + (I_t - I_e) \cdot \dot{\theta} \cdot cos\theta \cdot \dot{\phi} = -r \cdot (F_x \cdot cos\theta \cdot sin\phi + F_y \cdot cos\phi \cdot cos\theta - C \cdot sin\theta \cdot \dot{\phi}) \tag{6}$$

$$k_2 : I_e \cdot (-\dot{\theta} \cdot sin\theta \cdot \dot{\phi} + \ddot{\phi} \cdot cos\theta) = 0 \tag{7}$$

They were derived in order to find an analytical model of the system, however, since the experimentation of the prototype was prioritized, there was no time left for the model.

The prototype was 3D printed in PLA with an "Ultimaker 3" printer of the versatility due to the technique. Three different configurations were made. All of them involved a base with 29 neodymium, nickel-plated magnets, fixed in it. They were 5 mm thick and 9 mm in diameter with a magnetization degree equal to N50 [6]. The orientation of the magnets was chosen in an attempt to maximize the varying magnetic flux across the coils by alternating north and south orientations radially as it can be seen in figure 7.

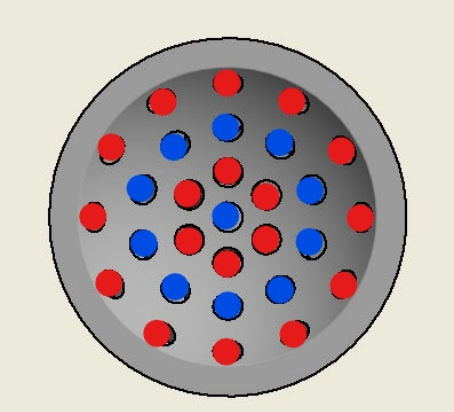

Figure 7: Orientation of the magnets in the bowl-based pendulum as seen from above. Red shows south orientation and blue, north orientation.

The three different configurations can be seen in figure 8. The 1-coil is the most simple, it consist sof one coil hanging by a string from a fixed point connected to the base. The coil was from"jantzen audio" made of copper wire with an internal resistance and inductance of 1.6 Ωand 0.35mH. It was 10 mm high with an inner diameter of 18 mm and outer diameter of25 mm. A more complex configuration was realized by designing a holder for the coils in which four coils, connected in series, were swinging. In this case, the coils chosen were more slender than previously, so they were better distributed in the holder. This configuration was thought so more flux could go through the coils, in principle generating more power. The last configuration consisted of eight coils (8-coils configuration) in series placed vertically in a holder. This was done in an attempt to harvest even more power than with the 4-coils configurations.

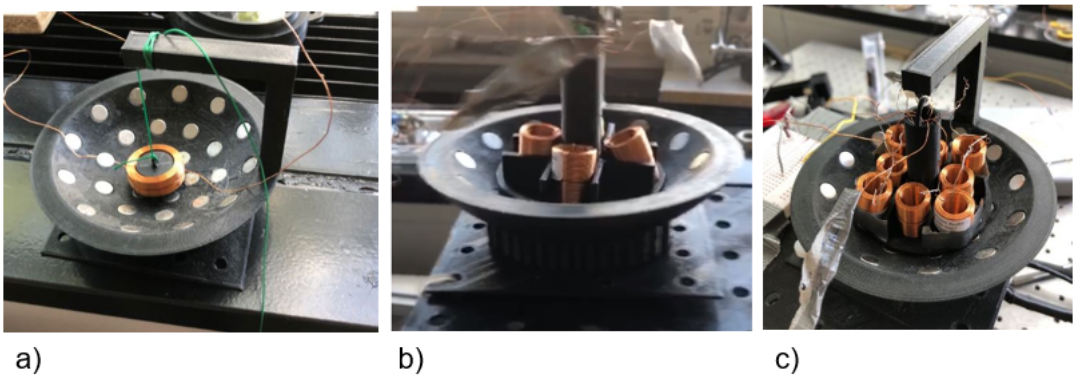

Figure 8: Three different configurations. a)1-coil b) 4-coils c)8-coils

3 Methodology

All the experiments were done following the same procedure: A 2-Dimensional electrodynamic shaker "H2W technology" were used to generate the vibrations. It was controlled by a LabVIEW interface. The output voltage was registered by a Data Acquisition and Control (DAC) system of National Instruments (NI USB-6351) of 16 channels. The output data was read from MatLab. (See figure 9).

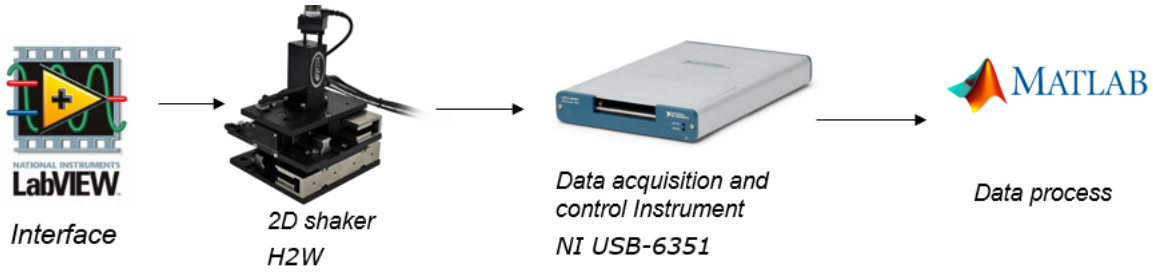

Figure 9: Methodology followed to make the experiments

The experiments were done with different vibration settings in 1D and 2D. Even though experiments in open circuit do not provide practical usage because no power is obtained, all the experiments were done in such way in order to see the limit of the system. Furthermore, for the vibration settings where the maximum output voltage happened in every device design, the experiments were repeated connecting the load that maximizes the power output, which is equivalent to the inner resistance of the system. This was done to compare the maximum output power between the different configurations.

4 Results

Figure 10 shows the Root Mean Square (RMS) of the voltage of all different configurations in the 1D study. It can be observed how 2 Hz is the natural frequency of the system since a maximum of voltage is found on it. Furthermore, the voltage tends to increase with the amplitude, which was expected because the displacement of the coils increases with the amplitude.

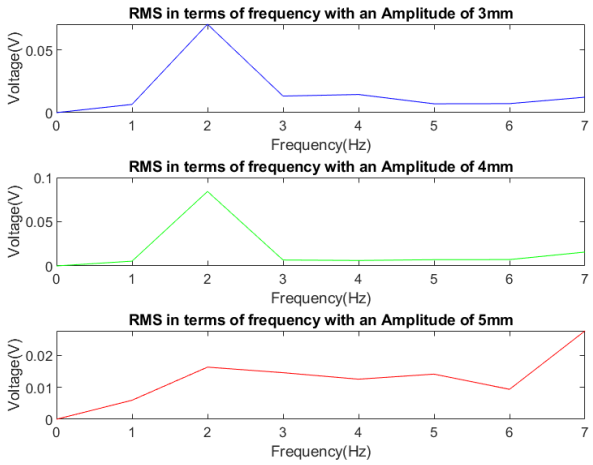

Figure 10: RMS in terms of frequency of the different configurations in open circuit with 1D vibrations

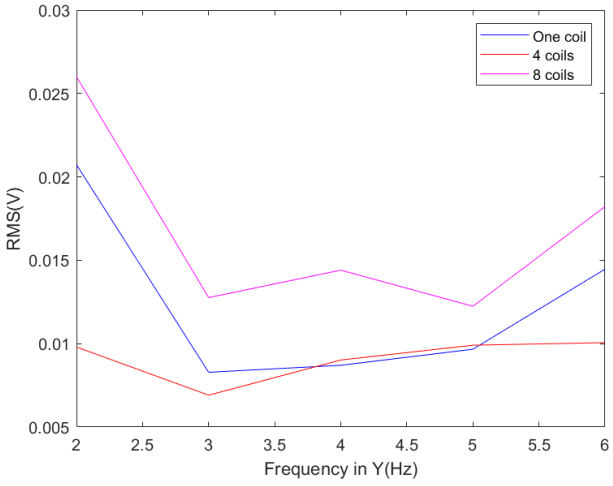

Figure 11: RMS with a 2-Dimensional horizontal vibration. In the "x" axis a constant amplitude of 3 mm and a frequency of 3 Hz and in the "y" axis, constant amplitude of 4 mm and varying frequency from 2 to 6 Hz.

It is seen that the 1-coil configuration provided almost the same RMS as the 8-coils and even more than the 4-coils arrangement. This can be due to two different things. First, the coils used for the 4-coils configuration are more slender, so less turns were concentrated close to the surface of the base, where most of the flux intensity appears. Second, since the coils are connected in series, their voltage may be out of phase cancelling each other and provoking lower output voltage.

Figure 11 shows the RMS of all the 2D experiments. The results of the 2D vibrations are similar to the ones in 1D.

Figure 12 shows the maximum RMS and power obtained in each configuration with the optimal load which is the equivalent to the inner resistance of the system in each case. The output power is calculated in the following way:

$$P = \frac{U_{rms}^2}{R} \tag{8}$$

where R is the load.

The maximum output power is 177 μW, with the one-coil configuration. It may be because of three things. First, the low inner resistance makes a much more efficient harvester. Second, the coil in this configuration is less slender, so there are more turns close to the surface, where most of the magnetic flux appears. And third, because in the 4 and 8 coils configurations, the voltage in each of the coils may be out of phase, reducing the final voltage.

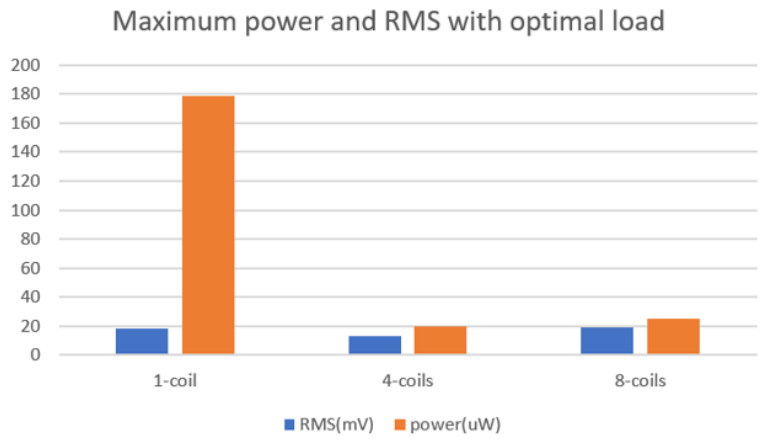

Figure 12: Maximum power and RMS obtained in every configuration loaded with its optimal resistance. With the vibration settings that provoked maximum voltage in open circuit, i.e. amplitude (x=5,y=0)mm, frequency (x=2,y=0)Hz for the 4-coils and 8-coils configurations and amplitude(x=3,y=4)mm, frequency(x=3,y=2)Hz for the 1-coil configuration.

5 Conclusions

This project presents a spherical pendulum design of an electromagnetic vibrations energy harvester and the experiments done to understand its behaviour. They show how the optimal configuration tend to be the one with the minimum inner resistance. The objectives of finding a 2D harvester with no mechanical friction are achieved. The maximum power obtained was enough to power ultra-low power devices. The system could be improved by increasing the intensity of the magnetic flux through the coils.

6 References

[1] Michael Vedomske. Without device longevity, the internet of things will never be.URLhttps://medium.co
the-grand-vision-of-the-internet-of/without-device-longevity-the-internet-of-things-will-never-
be-58c904703abb: :text

[2] BP Mann and ND Sims. Energy harvesting from the nonlinear oscillations of magneti-
clevitation.Journal of sound and vibration, 319(1-2):515–530, 2009.

[3] Krzysztof Kecik, Andrzej Mitura, Stefano Lenci, and Jerzy Warminski. Energy harvest-
ing from a magnetic levitation system.International Journal of Non-Linear Mechanics,94:200–206,
2017.

[4] Davide Castagnetti. A simply tunable electromagnetic pendulum energy harvester.Meccanica,
54(6):749–760, 2019.

[5] Magnetic properties of neudymium magnets. URLhttps://www.magnetexpert.com/magnetic-
properties-of-neodymium-magnets-i694.

[6] R Salazar, M Serrano, and A Abdelkefi. Fatigue in piezoelectric ceramic vibrationalenergy
harvesting: A review.Applied Energy, 270:115161, 2020.

Abstract

A fundamental issue for the "Internet of Things" (IoT) network is the battery replacement of wireless devices, which represents a big economical and environmental problem. To find a solution in this subject, different energy harvesting technologies are being developed. This project presents the experimental assessment regarding the friction of an already existing 2D electromagnetic vibration energy harvester (EMVEH) and the alternative found to solve the mechanical friction problems. This alternative consists of an spherical pendulum design, which aims to be a 2D harvester with no mechanical losses that can harvest energy in a broad band of low frequencies. The coils are positioned as the inertial mass and the base contains the magnets. The device was built with 3D printing because of the versatility of the technique. The equation of motion was derived using Newton-Euler´s equations. The harvester was tested in a 2D shaker with 1D and 2D vibrations obtaining information of the power and voltage generated by different set-ups of the pendulum. Finally, this results were compared so an optimal configuration was found.

Keywords: Energy harvesting. Internet of Things. Spherical pendulum. 2D. Friction. Vibrations.

Contents

1 Introduction

Internet of Things (IoT) is the network of devices that are continuously monitoring and sending information regarding the behaviour of physical objects, people, the environment or anything that provides any kind of data. Currently there are around 11 000 million devices connected in the network and is expected to triple in 5 years [7]. This is because of the improvement in the connectivity due to 5G and the increasingly need of gathering data for commercial purposes or the creation of the "smart cities" among other things.

A large proportion of these devices are wireless, therefore, they are fed by batteries. On average, the lifetime of these batteries is much smaller than the lifetime of the devices [1] . Consequently there is a great cost per year associated to the replacement and maintenance of the batteries not just because of their price itself but also because the logistics and workforce needed [8]. Moreover, there is also a big environmental damage related to the waste of the batteries. In order to solve this problem, different energy-harvesting technologies are emerging as an alternative IoT power source. This technologies are able to get energy from the environment via sunlight, thermal gradients or motion like vibration or wind among others. Specifically, this project will consist of investigating vibration energy harvesters, trying to optimize them and find out new possible designs for this kind of harvesters.

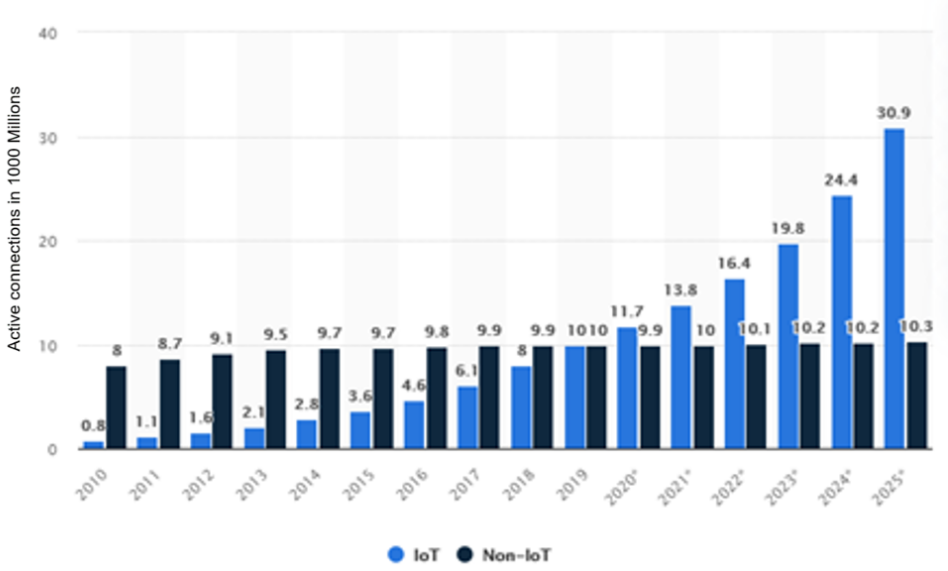

Figure 13: Evolution of number of IoT devices connected in the network. [7]

1.1 Impact of the work done

The energy-harvesting techniques have a meaningful impact environmentally and economically, enabling the IoT to be developed saving a lot of money, resources and energy. As it can be seen in Figure 13, in 2025 there are expected to be 30 900 million of IoT devices and supposed 70% of them wireless means 21 630 Million of wireless IoT devices.

The average lifetime of the batteries is 5 years [1], therefore, every year around 4300 Million batteries should be changed. The average price of a battery is 8$. It has been estimated by doing a market research of different buying platforms from different countries (Walmart.com, Mediamarkt.es, Elgiganten.dk, Rs.com) to have into consideration the different prices per country. Afterwards the price has been reduced a 30% because it has been appreciated the decrease in costs of bulk buying. Moreover, there is an additional cost due to the track rolls that make the maintenance and change of the batteries of the devices on the streets. This expense will consist of labour and vehicle costs and the opportunity-cost. Making the truck roll expense up to 150$ per battery change [9].

Considering all this, the total cost of changing the devices' batteries would be 675 100 Million $ per year. This huge expense to the IoT network is a great obstacle for the objective of living in smart cities and for being completely connected in the future. Not only the batteries replacement provoke a huge economic impact, but also significant environmental consequences. First, the manufacturing of the batteries. These batteries are made with different materials which mining is very polluting, such as lithium or nickel. This problem is worsen because of the increasingly need of lithium for the electric car batteries. therefore, every reduction in the use of lithium will mean a help for the environment. Second, the waste of the batteries represent a major problem. It is true that lead-acid batteries are highly recycled , however, other types like lithium-ion that are the ones being used for electric cars, among other things , are not usually recycled [10]. This waste pollutes a lot the environment being toxic for the near flora and fauna. Moreover, the amount of materials that has to be mined for the batteries is abusive, e.g., 85% of all the lead is used for this matter [11].

To sum up, the amount of resources and money that can be saved and the reduction of battery wastes that can be reached, make the energy harvesting a very interesting alternative for IoT power feeding. Consequently, this project is motivated by the desire of helping to make it possible.

1.2 Background

The main sources available for energy-harvesting are solar, electromagnetic radiation, thermal gradients, radio-frequency (RF) and motion. All have been studied and compared to some extent [12]. Photovoltaic (PV) panels are the most commercially established solution for a wide range of scales, primarily due to its low cost [13]. However, the inconsistency in the sun availability makes that for small scale harvesting is not a good solution [14]. Small-scale thermoelectric generation has been also widely studied and different successful applications such as the "Seiko Thermic Watch" have been developed . However, temperature differences tend to be small in scales at which the harvesters are built resulting in low efficiency. Some attention have also been received by ambient RF [15]. The key problems in this source are availability of meaningful power levels and the inefficient extraction using devices much smaller than the radiation wavelength [16]. The comparison between the different sources for energy including their advantages and disadvantages have been discussed by different authors [17], [18]. In general, the opinion in the literature is that, while each application should be evaluated independently in order to find the best method, kinetic energy in the form of vibrations is the most flexible and easily found ambient energy source available [19].

The most used technologies for small scale energy harvesting from motion are piezoelectric generators (PEGs) and electromagnetic energy harvesters [20]. Piezoelectricity is a property of certain crystalline materials such as quartz, Rochelle salt, tourmaline, and barium titanate that, when deformation or pressure is suffered, the electric charges within the crystal are unbalanced. This polarization can be used to generate a voltage and make electrical current run generating power [21]. Most piezoelectric energy harvesters are in the form of cantilever beams located on a vibrating structure. The dynamic strain results in an alternating voltage output [22]. The simplicity in its design [21], the low resistive losses [20] and the high power density [23] makes the piezoelectric a very interesting technology for harvesting energy. However, there is a key problem in PEGs, which is the degradation and potential crack of the material due to the fatigue suffered during its lifetime. [2].

Electromagnetic vibration energy harvesters (EMVEHs) use vibrations to create a relative movement between some magnets and coils. In that way, a varying magnetic flux would go through the coils, and therefore an alternating voltage is produced in them. This is explained by Faraday´s law [24]. The major advantages of this technology are the large adjustable range of parameters; the suitability for a large number of low frequency vibration in the environment and, unlike PEGs, the materials used can remain in a good condition indefinitely [25] [5]. Due to its easy parameter tuning, a lot of different designs of EMVEHs

have been built and modelled, for example magnetic levitation [3], [4] or diverse pendulum architectures [5] [26] [27].

To illustrate the concept of an EMVEH, consider the common basic architecture comprising a hollow cylindrical container, three or more permanent magnets forming a magnetic spring and one or more coils. The polarity of the magnets will be arranged in a way that the levitating magnet experiences a repulsive force due to the fixed magnet which are attached to the end extremities of the container (see Figure 14). With this design densities up to $8mW/cm^3$ have been achieved, and with harvesters of 235 cm^3 up to 43.4 V have been measured [28].

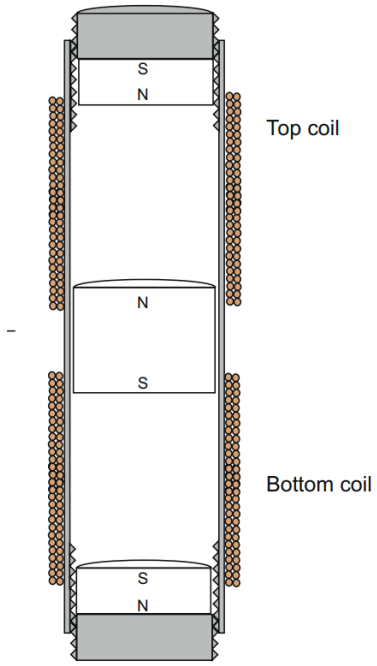

Figure 14: Typical magnetic levitation architecture in which the magnets are forming a magnetic sprig. [3]

A major problem found in the EMVEHs is the limitation of the frequency bandwidth. It is due to the fact that the resonant frequency of the generator has to be close to the one of the ambient vibration in order to achieve maximum power, otherwise it will decrease drastically [29]. To obtain a broader frequency band some authors propose pendulum design combined with electromagnetic transduction [30] [31]. However, these solutions involve considerably more complex architectures, consisting of many parts and a low energy output. A simpler design is found in Ref. [5] where a pendulum is combined with an adjustable magnetic spring

for which frequency tuning is achieved (See figure 15).

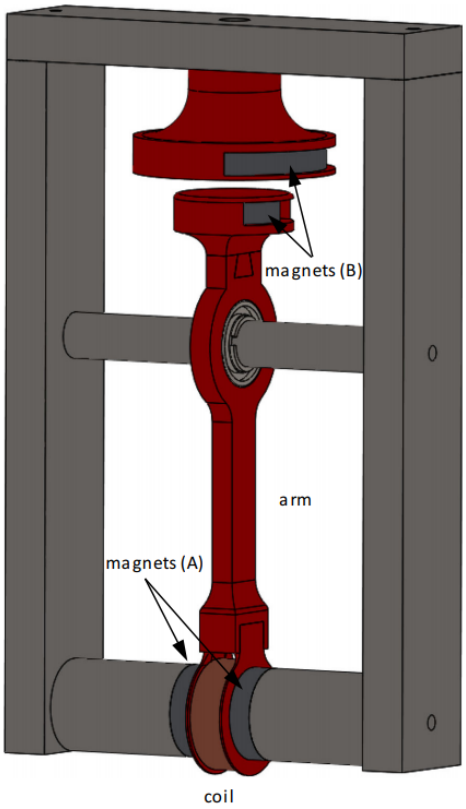

Figure 15: Harvester with frequency tuning designed by Ref. [5]

In some cases, like in train rails, the ambient vibration can appear in different directions [32], therefore, more-than-one-dimension harvesters are of great utility. However, not a lot of literature regarding this kind of EMVEHs is found. In Ref. [33] a design is presented. It consists of a free moving, axially magnetized disk magnet laying on a 2-dimensional plane with freedom of radial movement. Stationary axially magnetized cubic magnets are distributed around the circumference of the sidewall to form a magnetic-spring effect (See figure 16). The analysis of the harvested power was done for a vertically mounted design and with a mathematical model that considers the same expressions as for a 1D EMVEH. Therefore, the reason of employing this configuration was only to decrease friction but not scavenging energy from 2D vibrations.

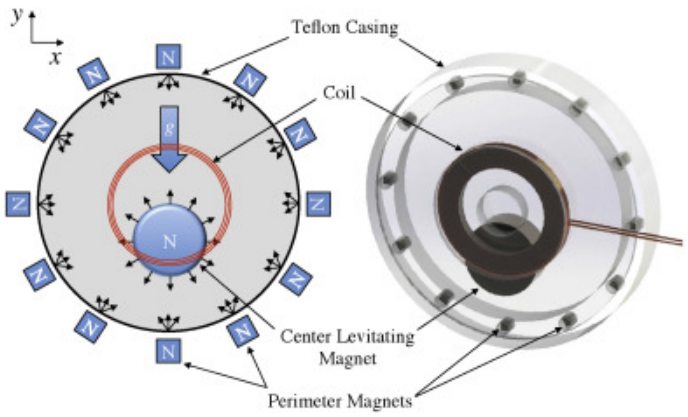

Figure 16: 2D EMVEH desgined by Ref. [33]

1.3 Objective

This works aims to study a 2D EMVEH designed by the Phd candidate Carlos Imbaquingo, and find solutions or alternatives for the friction problem, which was detected in previous studies. This experimental assessment lead to the idea of building another harvester. It consisted of a spherical pendulum in which the coils are positioned as the inertial mass and the base contains the magnets. It aims to be a simple 2D architecture, with no friction, that can harvest energy in a broad band of low frequencies. Different configurations of the design will be tested in a 2D-shaker in order to identify the optimal set-up. The output voltage and power of the pendulum will be studied with different frequencies and amplitudes.

2 Sustainable Development Goals

The Sustainable Development Goals consist of 17 objectives that address different challenges faced by the world, like poverty, inequality, climate change, peace and justice. They aim to achieve a better and more sustainable future for all [34].

Figure 17: Sustainable Development Goals aimed by this project.

The main goal related to this project is "Goal 7: affordable and clean energy" which looks for more sustainable and widely available energy. It is clearly connected to this projected since, an electromagnetic energy harvester used to power the IoT network would reduce the amount of batteries in use and consequently the damage in the environment produced by the manufacturing and waste. Furthermore, non-wireless devices could also be powered by electromagnetic energy harvesters and, in that way, the energy consumption of the grid would be reduced.

Other goal accomplished by this project is "Goal 11: Sustainable cities and communities". It is achieved since the increase of harvesters in the cities would reduced the consumption of energy. Furthermore, the existence of more accessible sensors for IoT would increase their presences in the cities. In this way, a growth in IoT devices will mean an improvement in the already existing smart cities, which aim for a maximum efficiency in terms of energy consumption, waste management and life quality for its citizens.

The powering of wireless devices by energy harvesters means a reduction in battery fabrication and battery replacement. There is a consequent decrease in the green house gases produced by, for example, the truck rolls or the lithium extraction for the batteries manufacturing. By reducing the green house gases, there is a considerable mitigation of the climate change, therefore, this project is also related with the "Goal 13: climate action".

3 Study of 2D Harvester

This chapter covers the brief study of the 2D harvester designed by Carlos Imbaquingo which he had tested and realized that at low frequencies, close to 4 Hz, the motion of the harvester is almost imperceptible. It was driven the hypotheses that the friction was causing the limitation of the movement. Therefore, different tests were realized in order to understand more the problem and verify the hypotheses.

The prototype consists of two parts. The first part is a two-ring magnetic structure which is free to move, with a set of coils located between the rings. The second part is a fixed system formed by a top and bottom plate with a set of cylindrical magnets placed at the center. Figure 4.1 shows the schematic f the 2D electromagnetic vibration energy harvester (EMVEH). The top lid of the prototype and the set of coils are not shown so that the internal parts can be seen.

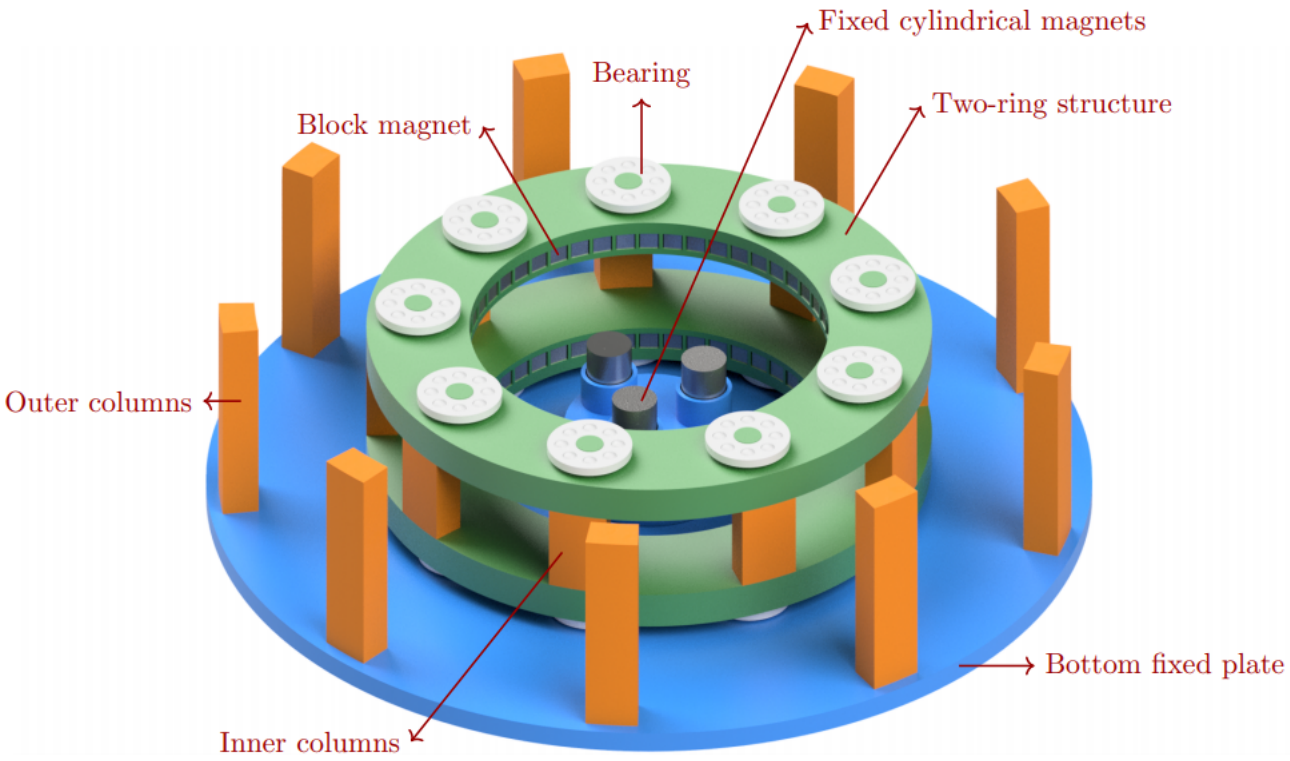

Figure 18: Schematic of Carlos Imbaquingo's EMVEH [35]

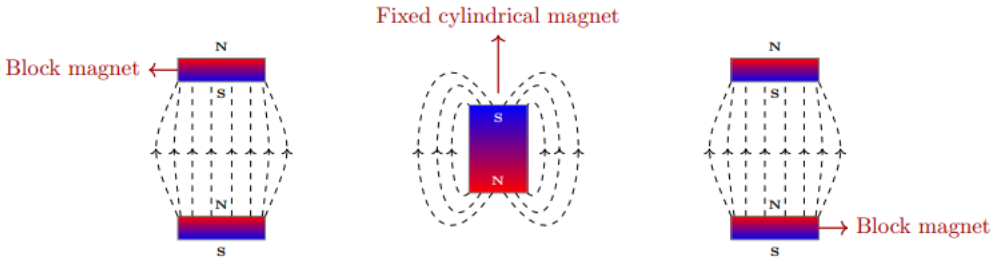

Figure 19: Cross-section of the 2-D EMVEH and magnetic flux lines between the two-ring structure (left and right) and fixed cylindrical magnet (center) [35]

When the prototype is exposed to ambient vibrations in one or more dimensions, the two-ring structure moves until the repulsive force, due to the interaction with the fixed cylindrical magnets pushes it back (see figure 19). The movement of the two-ring structure relative to the fixed cylindrical magnets simultaneously generates an electromagnetic force on the fixed winding coils that are located in the gap in the two-ring structure.

3.1 Study of the harvester

The first step was to quantify the mechanical friction of the two-ring structure. To do so, it has to be isolated from the fixed permanent magnets so there is not electromagnetic interaction. To know the static and dynamic friction coefficients the Coulomb‘s Friction experiment is done (see figure 20). It consists of pulling the structure with a string connected to a mass hanging from a pulley. The mass is increased until the structure moves. The friction force, F_f, is equal to the minimum mass required to move the structure, times the gravitational constant (9.81 m/s^2).

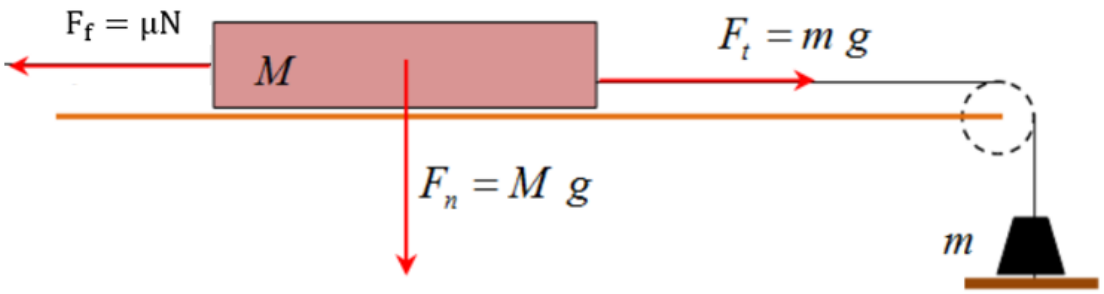

Figure 20: Coulomb‘s Friction experiment [36]

The mass of the moving structure is 290 g and it was needed 35 g to move it, therefore, the friction coefficient, μ, is calculated using the following equation:

$$F_f = \mu N \tag{9}$$

In that way, the static friction coefficient is $\mu_s = 0.12$, thus, the friction force is 0.34 N, and the acceleration of the external vibration required to motion the two-ring structure is 1.17 m/s^2, without considering the electromagnetic interaction with the fixed magnets.

The dynamic friction coefficient is also obtained so it is known the energy loses of the system once the harvester is moving. It is estimated using the same experiment but with a mass larger than the minimum required for the motion. The two-ring structure will cover a certain distance in a certain time. In that way, the coefficient can be obtained using the equation 9 and the notation in Figure 20. Thus:

$$F_t - F_f = Ma_M \tag{10}$$

Also,

$$x = \int\int adtdt \Rightarrow x = \frac{at^2}{2} \Rightarrow a = \frac{2x}{t^2} \tag{11}$$

Being x the certain distance covered and t the time the structure took to cover that distance.

Putting together equations 9, 10 and 11, the friction coefficient is derived, $\mu_d = 0.11$. Therefore, the friction force when the structure is moving is 0.31 N

The experiments were done three times to obtain more accurate results. There was a small standard deviation (0.002) showing the accuracy of the results.

The harvester is studied in a range of accelerations from 4 to 10 m/s^2 approximately, assuming an average of 7 m/s^2 , it means that the force suffered by the harvester is approximately 2 N. In that way, considering that the friction force is constant, the friction losses represents around 15% of the total input energy.

3.2 Tried Solution: Magnetic Levitation

To reduce the problems caused by the friction force, magnetic levitation is proposed. It is inspired by the 1D harvester in figure 14. The possible solution consisted of placing the two-ring structure between two magnetic plates of opposite polarization (see figure 21). In that way there would not be any kind of friction.

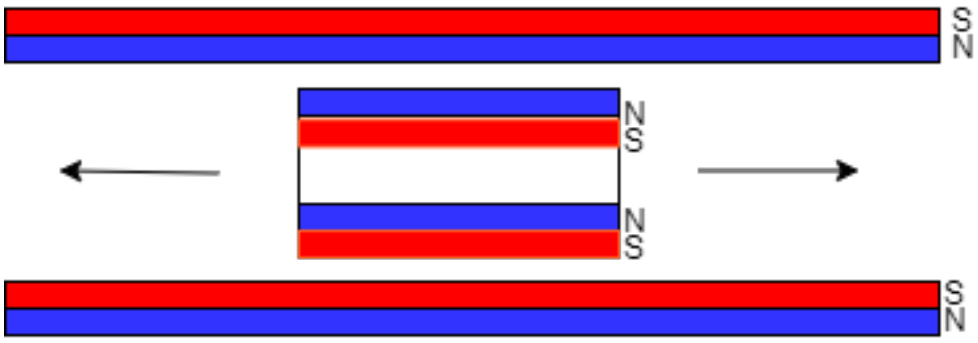

Figure 21: Idea of Magnetic Levitation Structure

However, the application of this solution was not physically possible. The reason of this is explained by the Earnshaw's theorem [37] which states that a body cannot be maintained in a stable equilibrium configuration with the only interaction of magnetic fields. Therefore there should be any degree of freedom constrained as it happens in the 1D model in which the magnetic torque makes the magnet bend and it is supported by the walls of the cylindrical container.

Nevertheless, there are two ways of obtaining magnetic levitation [37]. First, by having a variable magnetic field that maintains the equilibrium in the system [38]. The major inconvenience on this method is that a control system is required increasing significantly the costs and complexity of the mechanism. Moreover, it would require an additional cost of energy, which does not match with the objectives of the harvester.

On the other hand, a cheaper and more simple way to achieve magnetic levitation is with a permanent magnet and a diamagnetic material. When an external magnetic field is applied to these materials, a weak magnetic dipole moment is induced in the direction opposite to the applied field provoking a repulsion between the material and the magnet. Some diamagnetic materials are bismuth, carbon or lead. However, since the induced magnetic dipole in these

kind of materials is weak, the magnetic force produced is considerably low compared to the gravitational force [39]. In this way, the amount of material needed to make the structure levitate would go way beyond the dimensions of the device.

3.3 Conclusion

The aim of this section was to fix the friction problem of the Carlos Imaquingo´s harvester in order to achieve a 2D EMVEH for low frequencies. No possible solution was found, however, the idea of a new harvester without mechanical friction came up. It consisted of the spherical pendulum design.

4 Pendulum Design and analysis

4.1 Conceptual design of the harvester

Figure 22 presents a simple solution for a 2-dimensional, low frequency electromagnetic vibration energy harvester(EMVEH). Having a pendulum configuration, the system provides close-to-zero mechanical friction. The conceptual design consists of a coil made of copper wire hanging by a thread connected to a fixed point relative to a bowl-shaped base. This base contains magnets inserted in its surface. When the coil swings relative to the base due to the horizontal vibration of the bowl, a variable magnetic field across the coils is provoked, and therefore, an alternating voltage is produced.

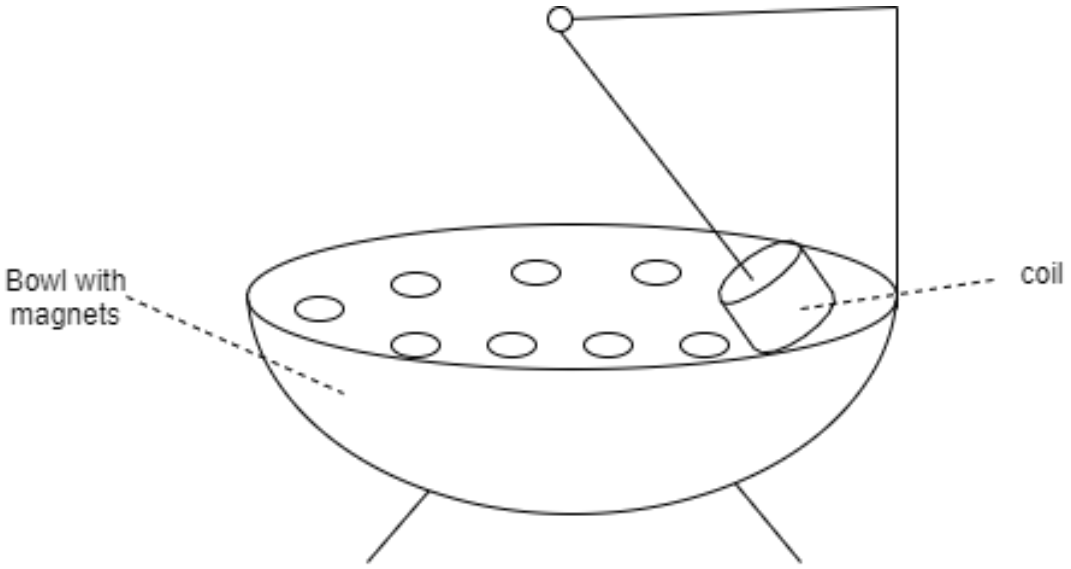

Figure 22: Conceptual design of the spherical pendulum EMVEH

4.2 Equations of motion

The equation of motion have to describe the behaviour of an spherical pendulum when an oscillatory external force is applied, considering the electromagnetic interactions. There are some challenges for solving the equation. First, the difficult geometry of the problem, in which the external forces are in the Cartesian coordinates(X,Y,Z) and the motion happens in the polar coordinates(θ, ϕ). Second, since there is an external force, the energy is not conserved, so no simplifications in the equations can be made. Third, the external force is

applied to the reference system, making it non-inertial, thus, inertial forces will appear [40].

The equations will be derived in the form Newton-Euler´s mechanics. They could be done using the Lagrangian mechanics which is easier mathematically, however, it is less intuitive than the Newtonian mechanics [41].

To derive the equations with Newton´s mechanics, Euler‘s angles have to be defined. Euler´s rotation theorem states that any rotation may be described using three angles: precession (ϕ), nutation (θ) and spin (ψ) (see figure 23). The transformation matrix regarding these three angles is E in the equation 12.

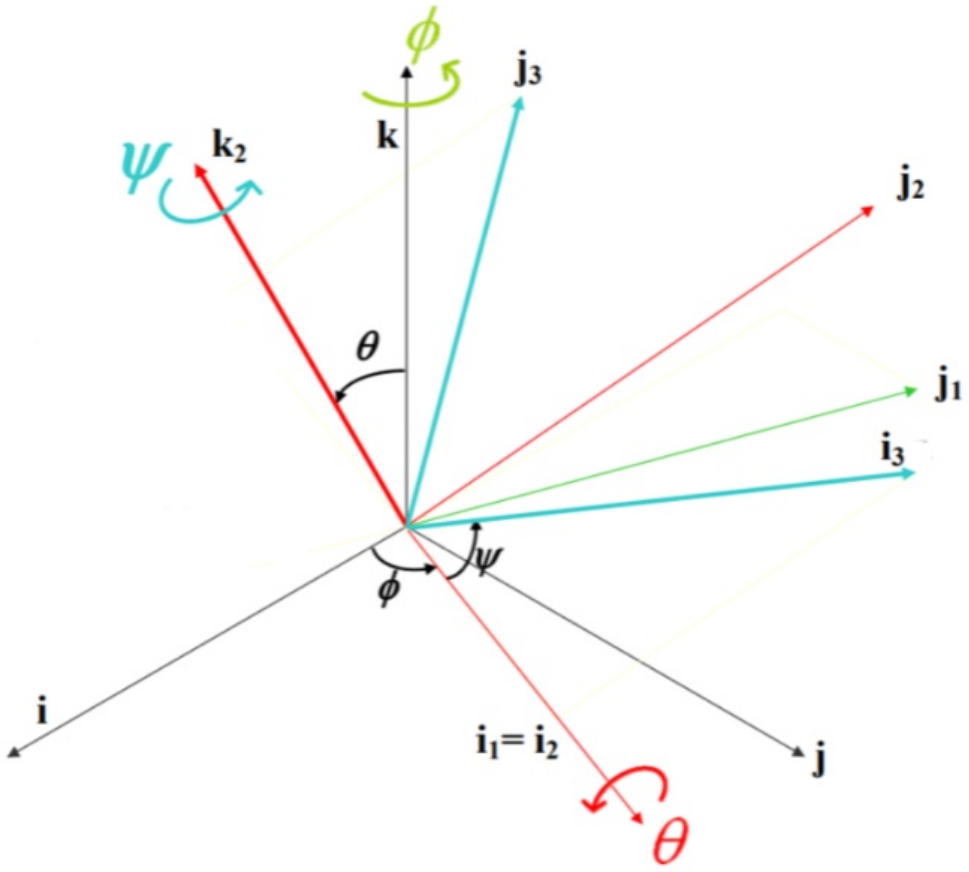

Figure 23: Transformation of the Cartesian coordinates when the Euler´s rotations are applied.

Figure 23 describes how the Cartesian coordinates (i,j,k) in black color are affected by the three Euler rotations, and shows the new coordinates systems ("System 1", "System 2", "System 3") that appear after the transformations. Precession (ϕ) is the rotation around the constant k axis, in that way the Cartesian coordinates are transformed into System 1 (i_1, j_1, k_1). Then, nutation, (θ) happens around the axis i_1 which is the former axis i being turned a certain angle ϕ. When nutation happens, the coordinates are transformed into System 2 (i_2, j_2, k_2). Last rotation is spin, when the System 2 rotates around k_2 to form the System 3 (i_3, j_3, k_3). Everything is defined by the transformation matrix in equation 12.

$$E = \begin{bmatrix} cos\psi cos\phi - cos\theta sen\phi sen\psi & cos\psi sen\phi + cos\theta cos\phi sen\psi & sen\theta sen\psi \\ -sen\psi cos\phi - cos\theta sen\phi cos\psi & -sen\psi sen\phi + cos\theta cos\phi cos\psi & sen\theta cos\psi \\ sen\theta sen\phi & -sen\theta cos\phi & cos\theta \end{bmatrix} \tag{12}$$

For solving the equation of motion of the pendulum, a system of coordinates that sees no variation in the geometry of the pendulum is aimed, thus, a system that rotates in conjunction to it. It is the case of "System 3". Having a constant geometry means that the moments of inertia are constant. It has been observed that there is not spin in the pendulum, therefore "System 2" is equivalent to "System 3". Figure 24 shows the motion of the pendulum represented by the Euler angles.

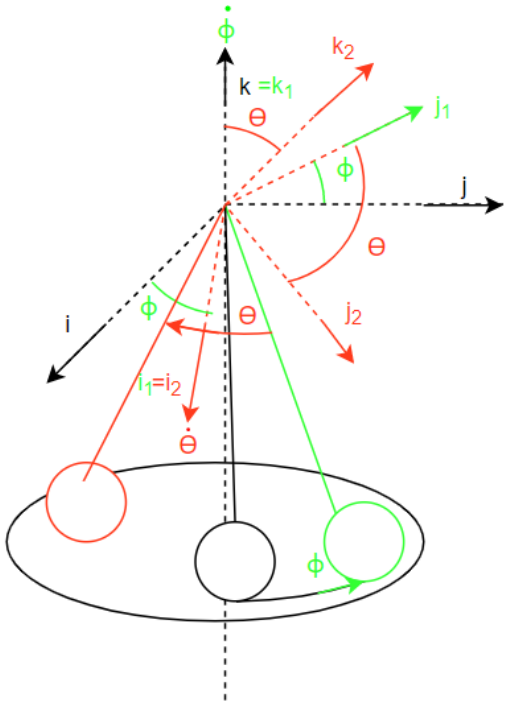

Figure 24: Motion of the pendulum represented by the Euler Angles

Considering the second newton law for rotation in 3 dimensions:

$$\overrightarrow{\tau} = \frac{\overrightarrow{dL}}{dt} = \frac{d}{dt}(II\omega) = II\frac{\overrightarrow{d\omega}}{dt} = II\overrightarrow{\alpha} \tag{13}$$

Where τ is the Torque, II is the inertial tensor, which is the matrix of moments of inertia, L is the angular momentum, α is the angular acceleration and ω is the angular velocity.

The inertial tensor using the "System 2" will be simplified because of the symmetry of the pendulum mass, in which the moments of inertia in the axis i_2 and j_2 are the same being $I_{i_2} = I_{j_2} = I_t$ and $I_{k_2} = I_e$. The moments of inertia are taken from the origin of coordinates seen in figure 24, which represents the joint of the string with the holder. In that way, the products of inertia, which are the non-diagonal terms of the matrix, are null. Thus the inertial II_2 is:

$$II = \begin{bmatrix} I_{i_2} & 0 & 0 \\ 0 & I_{j_2} & 0 \\ 0 & 0 & I_{k_2} \end{bmatrix} = \begin{bmatrix} I_t & 0 & 0 \\ 0 & I_t & 0 \\ 0 & 0 & I_e \end{bmatrix} \tag{14}$$

The angular velocity (ω) in the using Euler angles is represented in the following way:

$$\overrightarrow{\omega} = \dot{\phi}\overrightarrow{k} + \dot{\theta}\overrightarrow{i_1} \tag{15}$$

Where each axis of rotation is multiplied by the angular rotation that it generates.

The angular velocity in "system 2" is aimed, therefore, k and i_1 are expressed in the coordinates of "System 2".
Since $i_1 = i_2$, in "System 2":

$$\overrightarrow{i_1} = \begin{pmatrix} 1 \\ 0 \\ 0 \end{pmatrix} \tag{16}$$

and k in System 2:

$$\overrightarrow{k} = E \begin{pmatrix} 0 \\ 0 \\ 1 \end{pmatrix} = \begin{pmatrix} 0 \\ sin\theta \\ cos\theta \end{pmatrix} \tag{17}$$

Therefore the angular velocity in "System 2" is:

$$\overrightarrow{\omega_2} = \begin{bmatrix} \dot{\theta} \\ sin\theta \cdot \dot{\phi} \\ cos\theta \cdot \dot{\phi} \end{bmatrix} \tag{18}$$

It is known that the external momentum is equal to the external force cross product the radius:

$$\overrightarrow{\tau_{ext}} = \overrightarrow{F_{ext}} \times \overrightarrow{r} \tag{19}$$

The radius is the distance between the origin of coordinates to the center of mass. In the coordinates of "System 2" is:

$$\overrightarrow{r} = \begin{pmatrix} 0 \\ 0 \\ -r \end{pmatrix} \tag{20}$$

The external forces are applied in the x and y direction of the Cartesian coordinates so they are transformed to "System 2":

$$\overrightarrow{F_{ext2}} = E \cdot \overrightarrow{F_{ext}} = \begin{bmatrix} F_x \cdot cos\phi + F_y \cdot sin\phi \\ F_x \cdot cos\theta \cdot sin\phi + F_y \cdot cos\phi \cdot cos\theta \\ -F_y \cdot sin\theta \cdot cos\phi \end{bmatrix} \tag{21}$$

Last, there is an interaction between the magnets and the copper in the coils that provokes a damping. This damping will appear in the form of a damping coefficient "C" times the linear velocity, which is:

$$\overrightarrow{v} = \overrightarrow{\omega} \times \overrightarrow{r} = \begin{bmatrix} r \cdot \dot{\theta} \\ -r \cdot sin\theta \cdot \dot{\phi} \\ 0 \end{bmatrix} \tag{22}$$

Finally, putting together equations 13 to 21, the three equations that describe the motion of the pendulum are:

$$i_2 : I_t \cdot \ddot{\theta} + (I_e - I_t) \cdot sin\theta \cdot \dot{\phi} \cdot cos\theta \cdot \dot{\phi} = r \cdot (F_x \cdot cos\phi + F_y \cdot sin\phi - C \cdot \dot{\theta}) \tag{23}$$

$$j_2 : I_t \cdot (\dot{\theta} \cdot cos\theta \cdot \dot{\phi} + \ddot{\phi} \cdot sin\theta) + (I_t - I_e) \cdot \dot{\theta} \cdot cos\theta \cdot \dot{\phi} = -r \cdot (F_x \cdot cos\theta \cdot sin\phi + F_y \cdot cos\phi \cdot cos\theta - C \cdot sin\theta \cdot \dot{\phi}) \tag{24}$$

$$k_2 : I_e \cdot (-\dot{\theta} \cdot sin\theta \cdot \dot{\phi} + \ddot{\phi} \cdot cos\theta) = 0 \tag{25}$$

The solution of these equations should be done with the aid of computer programs, however, due to the limit in time, other things were prioritized in this project.

4.3 Configurations designed

Different configurations of the same prototype has been designed. All of them involved a base with 29 neodymium, nickel-plated magnets, fixed in it. They were 5 mm thick and 9 mm in diameter with a magnetization degree equal to N50 [6]. The dimensions of the prototype can be seen in figure 26. It was done in that size so it was easier to work with it while it could be scaled for the actual application. The orientation of the magnets was chosen in an attempt to maximize the varying magnetic flux across the coils by alternating north and south orientations radially as it can be seen in figure 25. The prototype was 3D printed in PLA with an "Ultimaker 3" printer. This technique was chosen because of its ease and versatility.

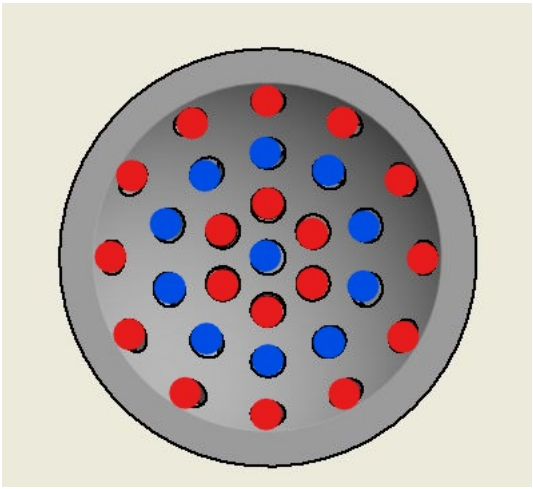

Figure 25: Orientation of the magnets in the bowl-based pendulum as seen from above. Red shows south orientation and blue, north orientation.

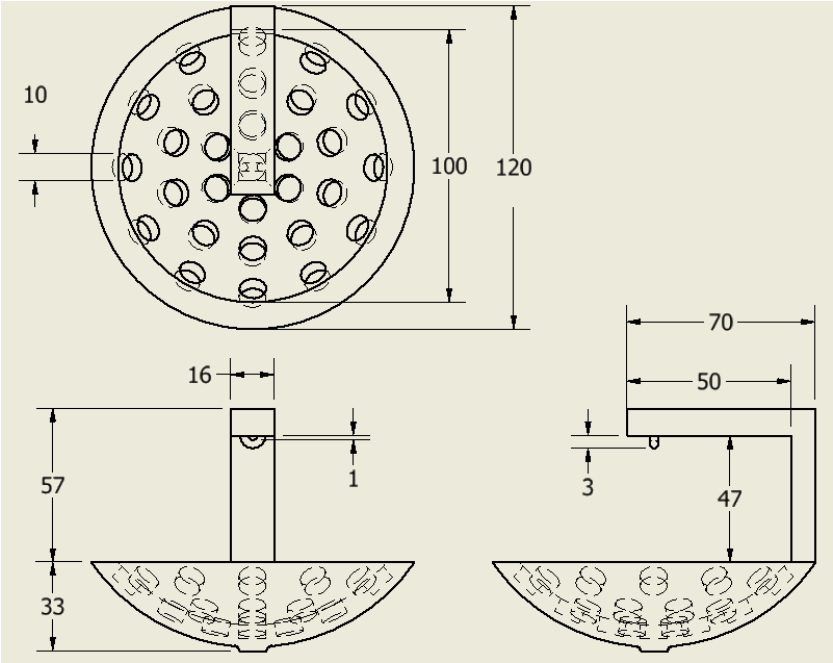

Figure 26: Sketch of the pendulum base with its dimensions (mm).

Figure 27 shows the most simple prototype built to proceed into the experiments. It consists of one coil hanging by a string from a fixed point connected to the base. The coil was from "jantzen audio" made of copper wire with an internal resistance and inductance of 1.6 Ω and 0.35 mH. It was 10 mm high with an inner diameter of 18 mm and outer diameter of 25 mm.

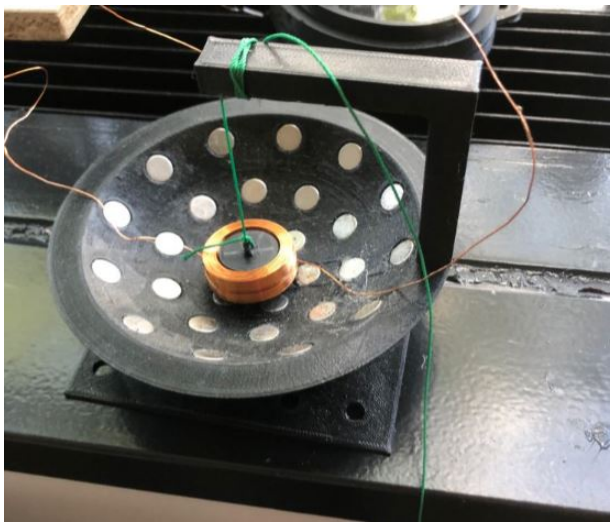

Figure 27: One coil configuration

A more complex configuration was realized by designing a holder for the coils in which four coils, connected in series, were swinging (see figure 28). In this case, the coils chosen had a similar impedance than before but were 21 mm high with and outer and inner diameters of 15 and 10 mm respectively, therefore they were more slender than previously, so they were better distributed in the holder. This configuration was thought so more flux could go through the coils, in principle generating more power. The coils orientation can be seen in figure 29. The last configuration consisted of eight coils in series placed vertically in a holder (see figure 29). This was done in an attempt to harvest even more power than with the 4-coils configurations.

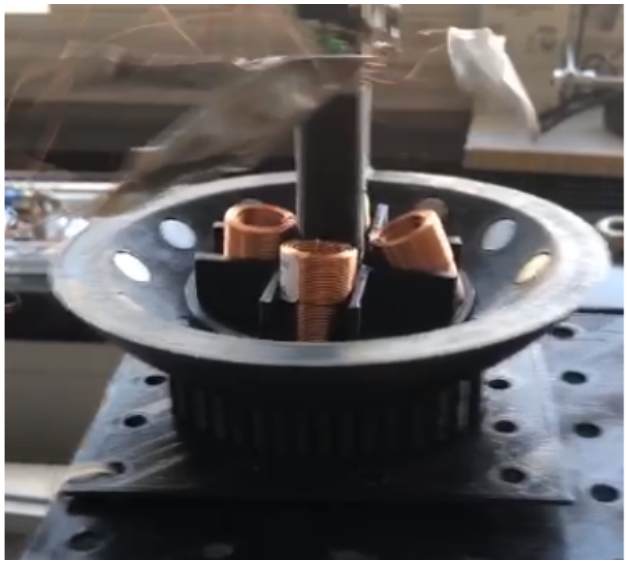

Figure 28: Pendulum configuration with four coils in series.

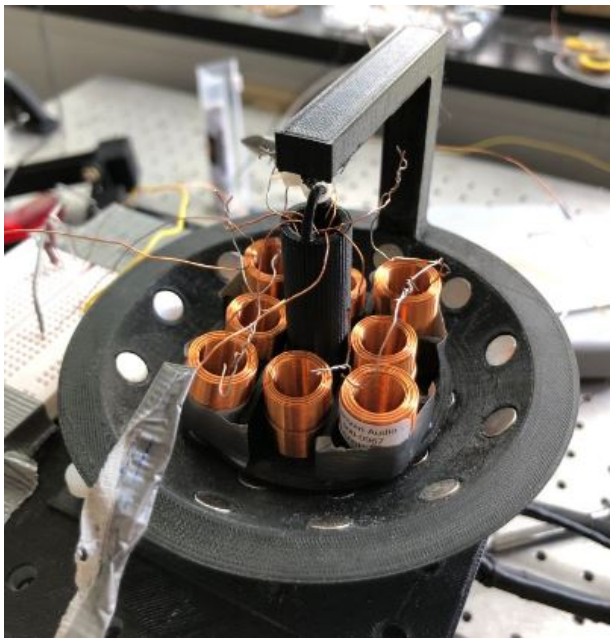

Figure 29: Pendulum configuration with eight coils in series.

4.4 Experimental Assessment

The experimental assessment involved the study of the configurations just described. Different vibrations in 1 and 2 dimensions were evaluated. In 1 dimension, the input vibrations tested had amplitudes of 3,4 and 5 mm and frequencies from 1 to 7 Hz discretely. Due to the large amount of degrees of freedom in the 2D vibrations, just a few generic vibrations were studied. The settings were in the "x" axis, a constant amplitude of 3 mm and a frequency of 3 Hz and in the "y" axis, constant amplitude of 4 mm and varying frequency from 2 to 6 Hz. Even though experiments in open circuit do not provide practical usage because no power is obtained, all the experiments were done in such way in order to see the limit of the system. Furthermore, for the vibration settings where the maximum output voltage happened in every device design, the experiments were repeated connecting the load that maximizes the power output, which is equivalent to the inner resistance of the system. This was done to compare the maximum output power between the different configurations.

A 2-Dimensional electrodynamic shaker "H2W technology" have been used to generate the vibrations. It was controlled by a LabVIEW interface. The output voltage was registered by a Data Acquisition and Control (DAC) system of National Instruments (NI USB-6351) of 16 channels. The output data was read from MatLab.

4.5 Results and discussions

All the data obtained from the experiments have been processed in order to filter the outliers. These outliers are punctual voltage registered that differs significantly from the rest of the signal and they were usually due to a bad connection between the DAC and the harvester that provoked a significant increase in the voltage. The connection was improved by plugging thicker wires into the DAC, however, the outliers did not disappear. Figure 15 shows the voltage of one of the configurations before and after the filtering.

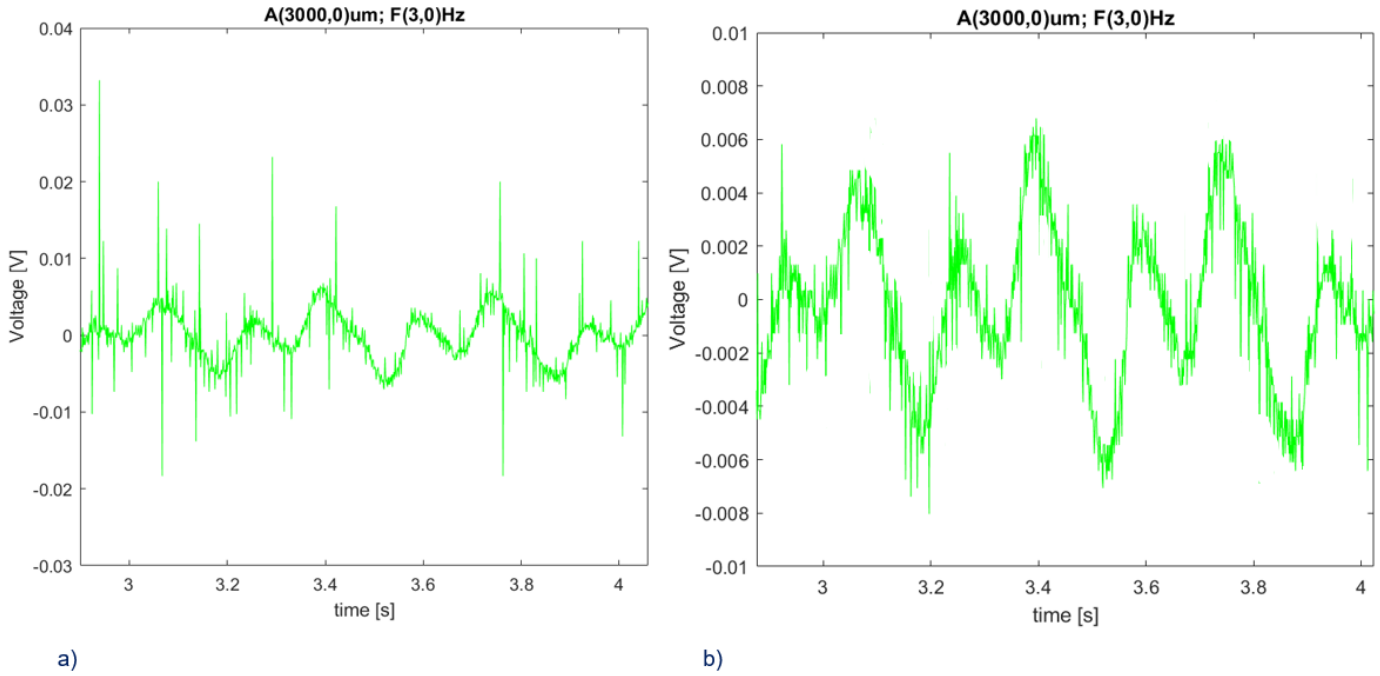

Figure 30: Example of filtering of outliers. a) Voltage originated from the raw data from the DAC. b) Voltage without outliers.

4.5.1 1D results

Figure 31 shows the Root Mean Square(RMS) of the voltage of all different configurations in the 1-Dimensional study. The RMS is plotted because it is the most representative single value of a signal. It is calculated in the following way:

$$U_{RMS} = \sqrt{\frac{1}{N}\sum_{k=0}^{N-1} u(k)^2} \tag{26}$$

Where N is the dimension of u, the voltage array.

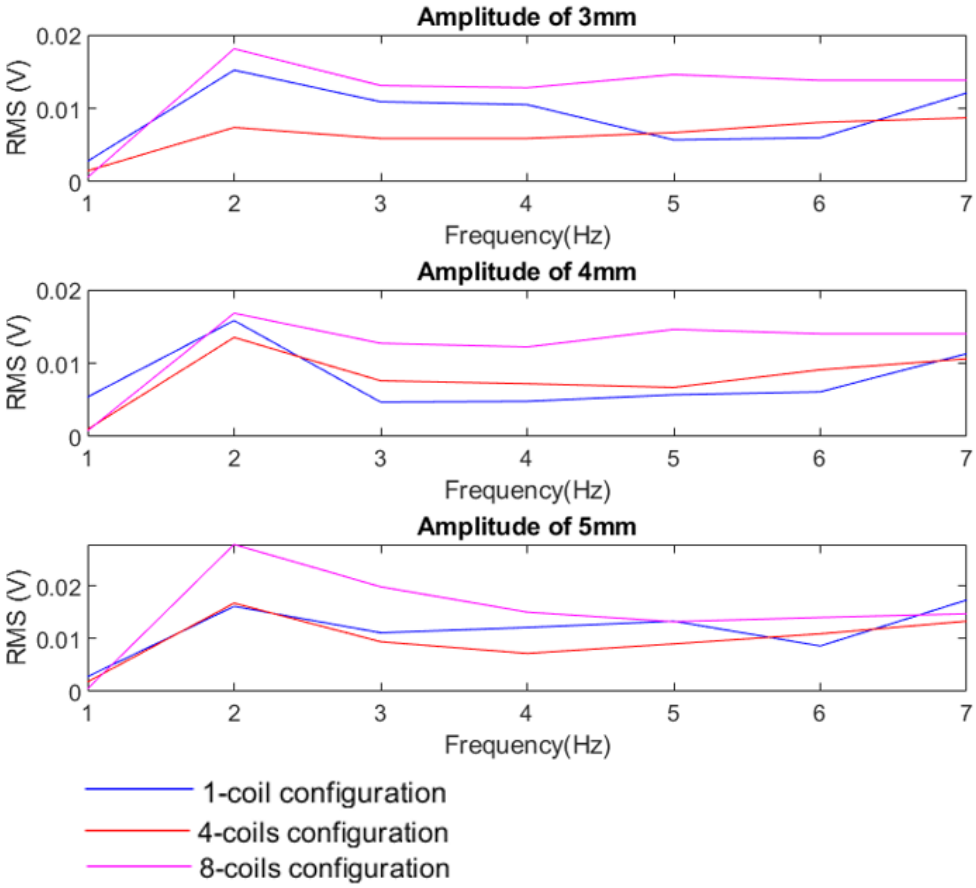

Figure 31: RMS in terms of frequency of the different configurations in open circuit.

Analysing figure 31, the following general conclusions are drawn. Almost no voltage is found with 1 Hz, while the maximum RMS appears in 2 Hz which implies that it is the natural frequency of the system. Furthermore, the voltage tends to increase with the amplitude, which was expected because the displacement of the coils increases as the amplitude does. It is interesting how there is not much variation between the voltage in the resonance frequency (2 Hz) and the rest of them even though it was observed much more motion of the pendulum with the resonance frequency. This is detailed in figure 32 where is seen that the effect of reaching the natural frequency for the output voltage is not increasing much the amplitude but rising the frequency and the harmonics of the signal. Since there is not much difference between the output voltage in the resonant frequency and the rest of frequencies, a broad band of frequencies is achieved.

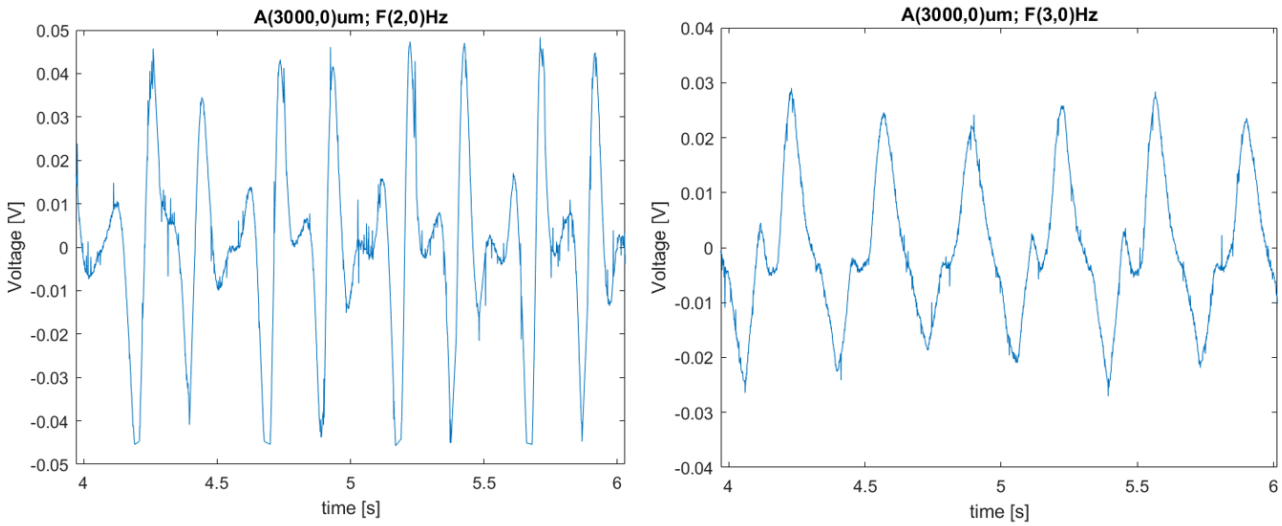

Figure 32: Two different voltage outputs of the 8 coils configuration

Focusing on the 1-coil configuration, there is a notable increase of the RMS in 7 Hz even though it is far from the natural frequency, moreover it was observed that there was almost not amplitude on the swing of the coil. However, the coil was rotating from the joint with the string (see figure 33) which provoked an alternative relative motion between the coil and the magnets, increasing the variation of the magnetic flux through the coils and therefore, the output voltage.

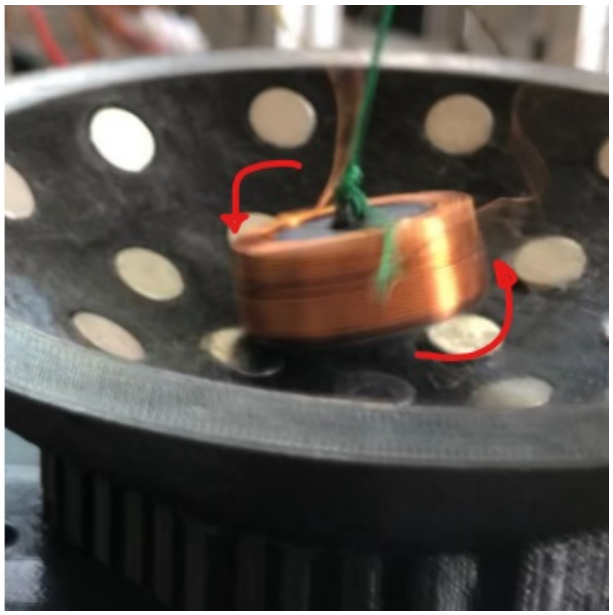

Figure 33: Rotation of the coil when a vibration of 7 Hz is suffered.

It is seen that the 1-coil configuration provided almost the same as the 8-coils and even more than the 4-coils arrangement. This can be due to two different things. First, the coils used for the 4-coils configuration are more slender, so less turns were concentrated close to the surface of the base, where most of the flux intensity appears. Second, since the coils are connected in series, their voltage may be out of phase cancelling each other and provoking lower output voltage. It can be seen in figure 34, where at some frequencies the different voltage are on phase and at others, out of phase.

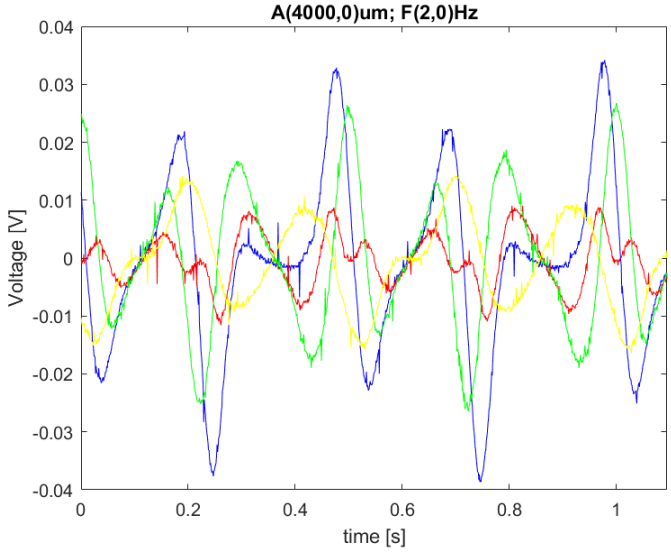

Figure 34: Voltage of the 4 coils configuration studied independently. Each color shows the voltage generated by a different coil.

4.5.2 2D results

Figure 35 shows the RMS of all the 2D experiments done with the settings mentioned in part 4.4. The results of the 2D vibrations are similar to the ones in 1D. However, it has to be remarked the minimum found in 3 Hz, this can be due to the fact that the frequency is the same in both axis. With this setting the pendulum swings just in circles and, due to the orientation of the magnets seen in figure 25, the variation of the magnetic flux is less than in radial swings, which is how it would swing in 1D. In the rest of 2D vibrations, the motion was a combination between radial and circular without any pattern observed.

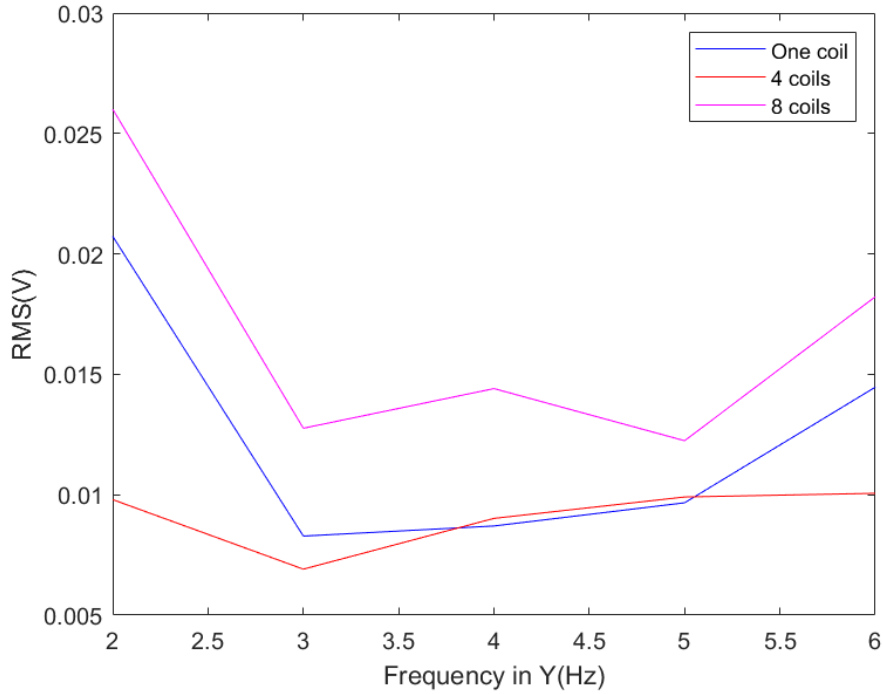

Figure 35: RMS with a 2-Dimensional horizontal vibration. In the "x" axis a constant amplitude of 3 mm and a frequency of 3 Hz and in the "y" axis, constant amplitude of 4 mm and varying frequency from 2 to 6 Hz.

4.5.3 Power results

Figure 36 shows the maximum RMS and power obtained in each configuration with the optimal load. This load in each case is: 1.6 Ω in the one-coil configuration, 6.6 Ω for each of the 4-coils and 14 Ω for the 8-coils configuration. This loads are the equivalent to the inner resistance of the systems. The output power is calculated in the following way:

$$P = \frac{U_{rms}^2}{R} \tag{27}$$

where R is the load.

The maximum output power is 177 μW, with the one-coil configuration. It may be because of three things. First, the low inner resistance makes a much more efficient harvester. Second, the coil in this configuration is less slender, so there are more turns close to the surface, where most of the magnetic flux appears. And third, because in the 4 and 8 coils configurations, the voltage in each of the coils may be out of phase, reducing the total final voltage.

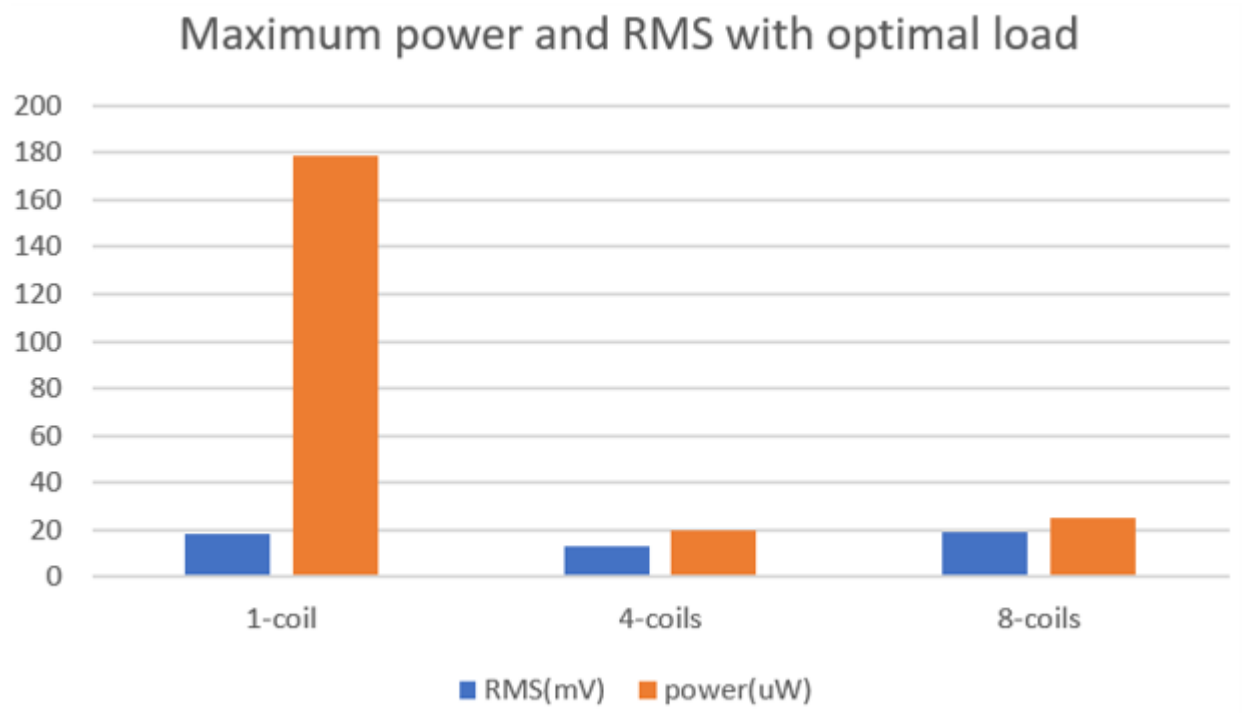

Figure 36: Maximum power and RMS obtained in every configuration loaded with its optimal resistance. With the vibration settings that provoked maximum voltage in open circuit, i.e. amplitude (x=5,y=0)mm, frequency (x=2,y=0)Hz for the 4-coils and 8-coils configurations and amplitude(x=3,y=4)mm, frequency(x=3,y=2)Hz for the 1-coil configuration.

4.5.4 Results into perspective

Overall, the output voltage and power are very low in comparison to other pendulum-design harvesters with similar dimensions seen in the literature [5] [27]. In those cases up to 9 mW were obtained, however the frequencies of the vibrations ranged around 20 Hz which makes a different study case. In Ref. [42] the power is studied with the same sort of frequencies as this one and it can obtain up to 748 $\mu W/cm^3$ while in this work not even $1\mu W/cm^3$ is harvested. However, the range of amplitudes are around ten times larger than in our case, and as said before in the work, bigger amplitudes usually relate to larger voltages, therefore, there cannot be a direct comparison between each other.

Anyway, the power generated is enough to feed ultra-low power devices [43]. Moreover, the objective of finding a 2D harvester with no mechanical friction that can harvest energy in a broad band of low frequencies is accomplished.

5 Conclusion

This project shows the study regarding the friction of an existing 2D electromagnetic vibration energy harvester (EMVEH). The experiments showed that the mechanical frictions was provoking high input energy losses. This study led to the idea of other 2D EMVEH design based on a spherical pendulum. This work presents the design, equations of motion and the experimental assessment of the pendulum harvester. The equations of motion were derived using the Newton-Euler's equations, however, the results have yet to be obtained with the aid of computer programs. The experiments were done for three different configurations of the pendulum harvester. They showed how the most efficient setting was the simplest, consisting of just one coil swinging close to the magnets. This was because different problems were found in the other set-ups, which comprised 4 and 8 coils respectively, connected in series. First, their high inner resistance provoked more losses; second, the more slender coils used, caused that less flux went through them; and third, the voltages produced by each coil independently were sometimes out of phase, provoking a cancellation between each other. In general, signals with a lot of harmonics were found. Moreover, the voltages tended to be higher at higher amplitudes. The power harvested was enough to feed ultra-low power devices. The system could be improved by increasing the intensity of the magnetic flux through the coils, for example, by adding more magnets in the top part of the pendulum. Further research could be done by realizing a computational model of the system so settings could be easily optimized and also, important parameters like the magnetic flux through the coils, could be quantified. Moreover, an interesting study would be to design and test a similar device in which the coils were fixed in the base and the magnets were the swinging mass, and compare the results with the ones obtained in this case.

References

[1] Michael Vedomske. Without device longevity, the internet of things will never be. URL https://medium.com/achieving-the-grand-vision-of-the-internet-of/without-device-longevity-the-internet-of-things-will-never-be-58c904703abb#:~:text=For%20most%20IoT%20applications%20the,to%2020%20years%20or%20more.&text=As%20applied%20to%20wireless%20technology,a%20long%20device%20life%20cycle.

[2] R Salazar, M Serrano, and A Abdelkefi. Fatigue in piezoelectric ceramic vibrational energy harvesting: A review. *Applied Energy*, 270:115161, 2020.

[3] BP Mann and ND Sims. Energy harvesting from the nonlinear oscillations of magnetic levitation. *Journal of sound and vibration*, 319(1-2):515–530, 2009.

[4] Krzysztof Kecik, Andrzej Mitura, Stefano Lenci, and Jerzy Warminski. Energy harvesting from a magnetic levitation system. *International Journal of Non-Linear Mechanics*, 94:200–206, 2017.

[5] Davide Castagnetti. A simply tunable electromagnetic pendulum energy harvester. *Meccanica*, 54(6):749–760, 2019.

[6] Magnetic properties of neudymium magnets. URL https://www.magnetexpert.com/magnetic-properties-of-neodymium-magnets-i694.

[7] Lionel Sujay Vailshery. Sujay: Iot and non-iot connections worldwide 2010-2025. URL https://www.statista.com/statistics/1101442/iot-number-of-connected-devices-worldwide/.

[8] Jerome P Lynch and Kenneth J Loh. A summary review of wireless sensors and sensor networks for structural health monitoring. *Shock and Vibration Digest*, 38(2):91–130, 2006.

[9] Hagai Shaham AR in Enterprise Posted on. Reduce your truck rolls costs: The surprising solution, 2020. URL https://techsee.me/blog/reduce-truck-rolls/#:~:text=What%20is%20a%20truck%20roll,other%20form%20of%20technical%20service.

[10] Lead vs. lithium battery recycling, 2018. URL https://wasteadvantagemag.com/lead-vs-lithium-battery-recycling/.

[11] Robert Rapier. Environmental implications of lead-acid and lithium-ion batteries, 2020. URL https://www.forbes.com/sites/rrapier/2020/01/19/environmental-implications-of-lead-acid-and-lithium-ion-batteries/#:~:text=According%20to%20the%20World%20Health,acid%20batteries%20are%2099%25%20recyclable.

[12] Neha Garg and Ritu Garg. Energy harvesting in iot devices a survey. In *2017 International Conference on Intelligent Sustainable Systems (ICISS)*, pages 127–131. IEEE, 2017.

[13] Daniel M Bennett, Richard H Selfridge, Paul Humble, and John N Harb. Hybrid power systems for autonomous mems. In *Smart Structures and Materials 2001: Smart Electronics and MEMS*, volume 4334, pages 354–362. International Society for Optics and Photonics, 2001.

[14] Yongliang Li, Sanjeeva Witharana, Hui Cao, Mathieu Lasfargues, Yun Huang, and Yulong Ding. Wide spectrum solar energy harvesting through an integrated photovoltaic and thermoelectric system. *Particuology*, 15:39–44, 2014.

[15] Matthai Philipose, Joshua R Smith, Bing Jiang, Alexander Mamishev, Sumit Roy, and Kishore Sundara-Rajan. Battery-free wireless identification and sensing. *IEEE Pervasive computing*, 4(1):37–45, 2005.

[16] Edwin D Mantiply, Kenneth R Pohl, Samuel W Poppell, and Julia A Murphy. Summary of measured radiofrequency electric and magnetic fields (10 khz to 30 ghz) in the general and work environment. *Bioelectromagnetics: Journal of the Bioelectromagnetics Society, The Society for Physical Regulation in Biology and Medicine, The European Bioelectromagnetics Association*, 18(8):563–577, 1997.

[17] Shad Roundy, Dan Steingart, Luc Frechette, Paul Wright, and Jan Rabaey. Power sources for wireless sensor networks. In *European workshop on wireless sensor networks*, pages 1–17. Springer, 2004.

[18] Thad Starner and Joseph A Paradiso. Human generated power for mobile electronics. *Low-power electronics design*, 45:1–35, 2004.

[19] Paul D Mitcheson, Eric M Yeatman, G Kondala Rao, Andrew S Holmes, and Tim C Green. Energy harvesting from human and machine motion for wireless electronic devices. *Proceedings of the IEEE*, 96(9):1457–1486, 2008.

[20] Emmanuelle Arroyo, Adrien Badel, Fabien Formosa, Yipeng Wu, and J Qiu. Comparison of electromagnetic and piezoelectric vibration energy harvesters: model and experiments. *Sensors and Actuators A: Physical*, 183:148–156, 2012.

[21] Heung Soo Kim, Joo-Hyong Kim, and Jaehwan Kim. A review of piezoelectric energy harvesting based on vibration. *International journal of precision engineering and manufacturing*, 12(6):1129–1141, 2011.

[22] Alper Erturk and Daniel J Inman. *Piezoelectric energy harvesting*. John Wiley & Sons, 2011.

[23] G Poulin, E Sarraute, and F Costa. Generation of electrical energy for portable devices: Comparative study of an electromagnetic and a piezoelectric system. *Sensors and Actuators A: physical*, 116(3):461–471, 2004.

[24] Edward C Jordan and Keith G Balmain. Electromagnetic waves and radiating systems. 1968.

[25] Yushan Tan, Ying Dong, and Xiaohao Wang. Review of mems electromagnetic vibration energy harvester. *Journal of Microelectromechanical Systems*, 26(1):1–16, 2016.

[26] James Graves, Yang Kuang, and Meiling Zhu. Scalable pendulum energy harvester for unmanned surface vehicles. *Sensors and Actuators A: Physical*, 315:112356, 2020.

[27] Bartłomiej Ambrożkiewicz, Grzegorz Litak, and Piotr Wolszczak. Modelling of electromagnetic energy harvester with rotational pendulum using mechanical vibrations to scavenge electrical energy. *Applied Sciences*, 10(2):671, 2020.

[28] Pedro Carneiro, Marco P Soares dos Santos, André Rodrigues, Jorge AF Ferreira, José AO Simões, A Torres Marques, and Andrei L Kholkin. Electromagnetic energy harvesting using magnetic levitation architectures: A review. *Applied Energy*, 260:114191, 2020.

[29] Chongfeng Wei and Xingjian Jing. A comprehensive review on vibration energy harvesting: Modelling and realization. *Renewable and Sustainable Energy Reviews*, 74:1–18, 2017.

[30] Tian-Wei Ma, Hui Zhang, and Ning-Shou Xu. A novel parametrically excited non-linear energy harvester. *Mechanical Systems and Signal Processing*, 28:323–332, 2012.

[31] Arnaud Notué Kadjie and Paul Woafo. Effects of springs on a pendulum electromechanical energy harvester. *Theoretical and Applied Mechanics Letters*, 4(6):063001, 2014.

[32] Z Li. Squats on railway rails. In *Wheel–rail interface handbook*, pages 409–436. Elsevier, 2009.

[33] Manuel Gutierrez, Amir Shahidi, David Berdy, and Dimitrios Peroulis. Design and characterization of a low frequency 2-dimensional magnetic levitation kinetic energy harvester. *Sensors and Actuators A: Physical*, 236:1–10, 2015.

[34] United Nations. Sustainable development goals.

[35] DTU Energy. Continuous modelling and testing, 2020.

[36] What is the coulomb's friction law, 2020. URL `https://www.encyclopedie-environnement.org/en/zoom/what-is-the-coulomb-friction-law/`.

[37] EMIL Cazacu and A Moraru. Escaping from earnshaw's theorem. *REVUE ROUMAINE DES SCIENCES TECHNIQUES SERIE ELECTROTECHNIQUE ET ENERGETIQUE*, 51(3):275, 2006.

[38] Donald M. Rote. Magnetic levitation. In Cutler J. Cleveland, editor, *Encyclopedia of Energy*, pages 691–703. Elsevier, New York, 2004. ISBN 978-0-12-176480-7. doi: https://doi.org/10.1016/B0-12-176480-X/00182-0. URL `https://www.sciencedirect.com/science/article/pii/B012176480X001820`.

[39] MD Simon and AK Geim. Diamagnetic levitation: Flying frogs and floating magnets. *Journal of applied physics*, 87(9):6200–6204, 2000.

[40] Encyclopedia Britannica. Inertial forces.

[41] Douglas Cline. The lagrangian versus the newtonian approach to classical mechanics, 2020. URL `https://phys.libretexts.org/@go/page/14065`.

[42] Yecheng Shen and Kaiyuan Lu. Scavenging power from ultra-low frequency and large amplitude vibration source through a new non-resonant electromagnetic energy harvester. *Energy Conversion and Management*, 222:113233, 2020.

[43] Jacob Borgeson, Stefan Schauer, and Horst Diewald. Benchmarking mcu power consumption for ultra-low-power applications. *Texas Instruments*, 2012.